NASA Contractor Report 165422

Experimental Study of the Effects of Secondary Air on the Emissions and Stability of a Lean Premixed Combustor

Gerald Roffe and R. S. Venkat Raman
General Applied Science Laboratories, Inc.
Westbury, New York

Prepared for
Lewis Research Center
under Contract NAS3-21271

August 1981

TABLE OF CONTENTS

LIST OF FIGURES

LIST OF FIGURES (cont'd.)

INTRODUCTION

Lean premixed prevaporized (LPP) combustion is a technique with the potential to significantly lower thermal NO_x production in gas turbine engines. Recent concept studies (References 1 and 2) incorporating LPP combustion in operational gas turbine engines have proposed designs which make use of variable geometry devices to control the stoichiometry of the combustor primary zone. At idle, the secondary air ports would be increased while at take-off and cruise, the secondary ports would be decreased, forcing more air into the combustor primary zone. Design proposals also call for film cooling combustor wall regions downstream of the primary zone. To date, research on LPP combustion at gas turbine operating conditions has dealt primarily with the emissions and stability of combustor primary zones and has employed flame-tube type test fixtures. The purpose of the present study is to experimentally examine the interactions between an LPP primary zone and the various secondary airflows present in a gas turbine combustor.

Secondary airflow in a gas turbine combustor can be broadly divided into two categories: dilution airflow and liner cooling airflow. Dilution air is generally injected normal to the combustor liner and is intended to mix rapidly with the bulk of the primary zone effluent, thereby affecting both temperature and species profiles. Liner cooling air, on the other hand, is generally injected tangentially and is intended to mix rather slowly with the other gases in the combustor. Dilution air reduces the bulk gas temperatures, which in turn affect mainstream NO_x production and CO oxidation reactions. Liner cooling air produces similar effects, however, these effects are locally more pronounced due to the necessarily lower temperatures which must exist near the walls.

The recirculating flow regions immediately downstream of the flameholder, which stabilize LPP combustion systems, could entrain air from both dilution and cooling airflows. This entrainment has the effect of cooling and diluting the recirculating flow region, thereby affecting the stoichiometry of the reaction zone and the stability of the system.

The effects of secondary air addition on the emissions and stability

of an LPP gas turbine combustor have been studied experimentally in the program described here. Tests were conducted using a film-cooled, rectangular combustor test rig provided with two variable geometry dilution stages capable of passing up to 50% of the total combustor air-flow. The tests were conducted using two flameholder designs: a perforated plate, to represent the class of flameholder geometries whose flame-stabilizing recirculation zones are of relatively small downstream extent, and a vee gutter, to represent the class of flameholder geometries whose recirculation zones are of relatively large downstream extent.

Over the spectrum of dilution staging options, the system streamline geometry (pattern) for each flameholder was determined by cold flow testing at ambient pressure. At these same conditions, the extent of flameholder recirculation zone dilution was obtained by tracer gas testing. Finally, the emissions and stability characteristics of the system were determined by combustion testing over the range of stable fuel/air ratios for all geometries at the fixed inlet condition of 630K/0.5MPa with a combustor reference velocity of 30 m/s.

APPARATUS AND PROCEDURES

Figure (1) is a schematic illustration of the test apparatus used in this program. The assembly consists of an inlet instrumentation spool containing temperature and pressure rakes, a combustor housing containing the mixture preparation section, bypass ducts and combustion zone, an exit instrumentation spool containing temperature, pressure and gas sampling rakes, and finally, a pressure control section consisting of a back - pressure orifice and air injection system for pressure control. The entire device is connected to the GASL horizontal pebble bed heater which supplies dry heated air to the device. The air supply system mixes heated air from the pebble bed with cold bypass air to produce a constant outlet temperature. The heat storage capacity of the bed is sufficient to allow operation for periods up to 20 minutes.

The inlet and exhaust instrumentation rakes are illustrated in Figure (2). Two five-point rakes are used in the inlet section, each provided with two pitot pressure and three thermocouple probes. The exhaust section contains three water-cooled nine-point instrumentation rakes, each of which provides four pitot pressure and five combination sampling/thermocouple probes. The five gas sample lines from each rake are manifolded externally as shown in Figure (3). The three rake manifolds are then joined together to provide a mixed sample for exhaust gas analysis.

Figure (4) provides a more detailed view of the combustor section of the test apparatus. Air enters through a 6^{o} half-angle dump diffuser which connects the 100x100mm inlet section with the 100x200mm combustor section. The entering air is divided between the mixture preparation (mixprep) duct and the bypass duct. The mixprep duct is 400mm long measured from the entrance of the fuel injection assembly to the flameholder exit plane.

The hot section of the combustor is covered by film cooling plena which supply air to a series of six tangential injection slots which pass approximately 20% of the total combustor airflow, depending upon dilution

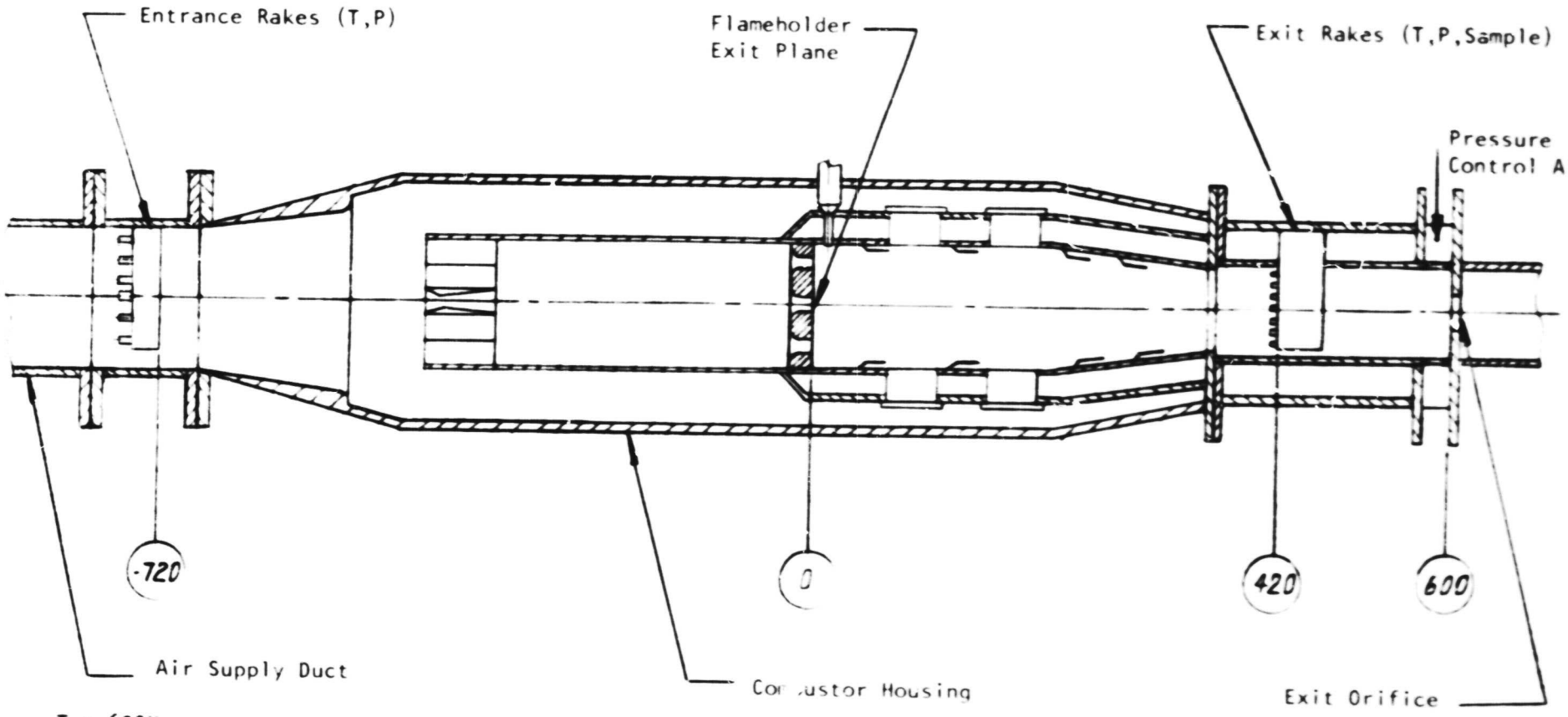

T = 630K
P = 0.5 MPa
V_{ref} = 30 m/s
$\dot{m}_{air}$ = 0.83 kg/s

Note: Circled numbers indicate distance from flameholder exit plane in mm.

FIGURE 1. OVERALL LAYOUT OF TEST RIG

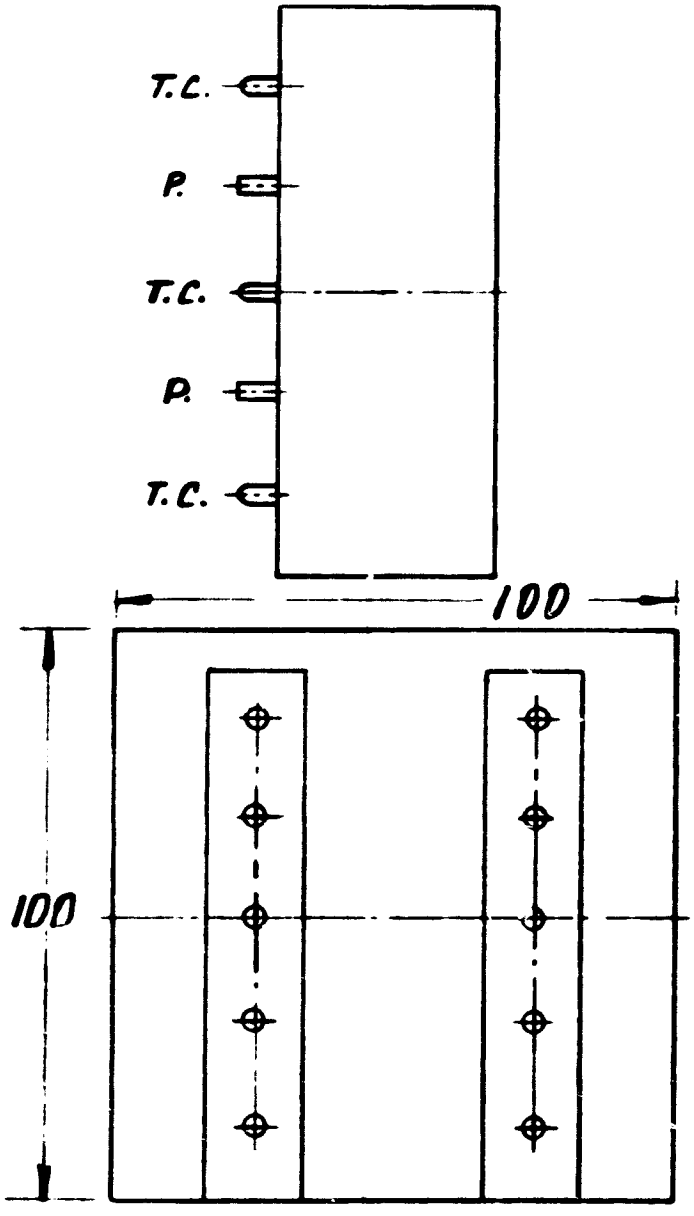

Inlet Rakes

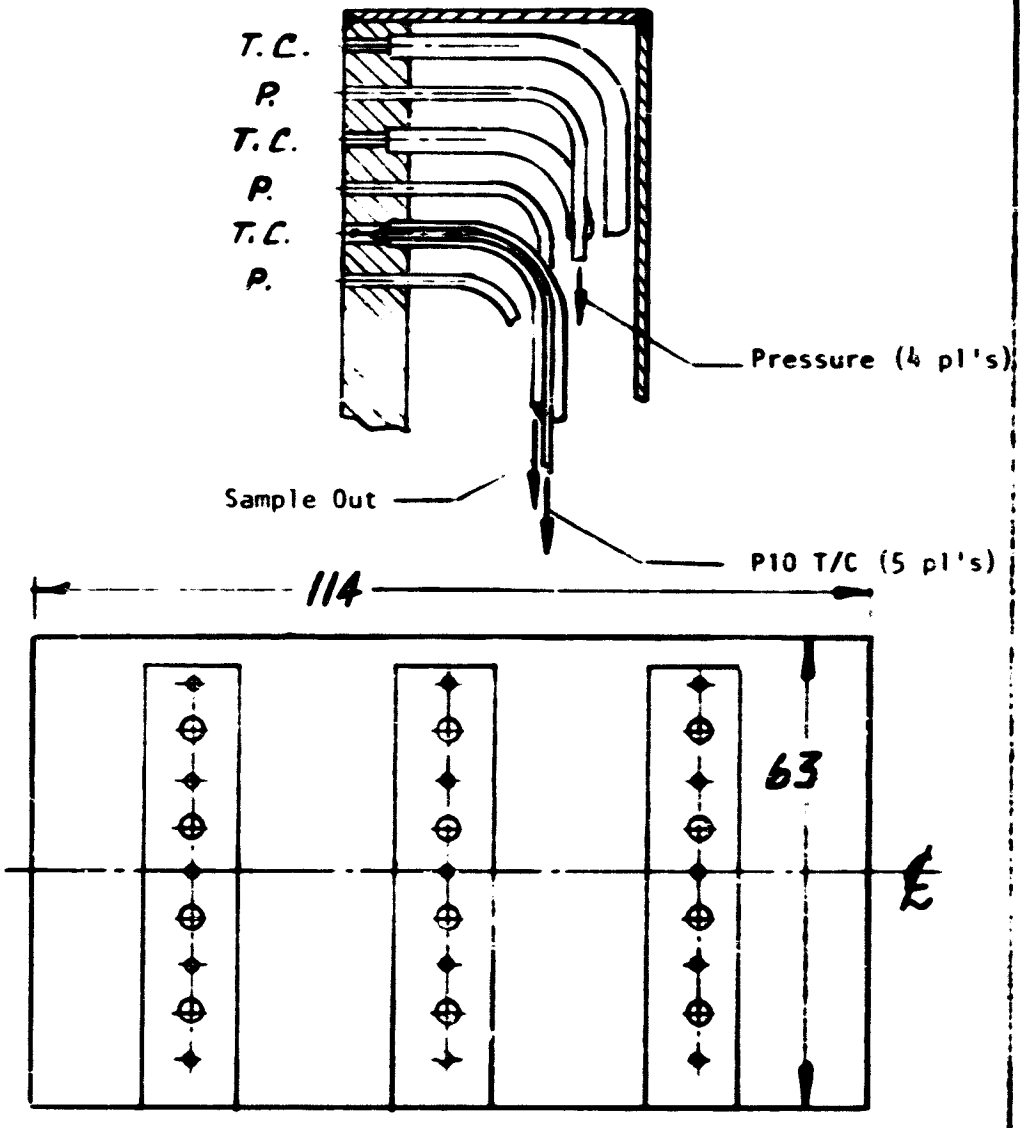

Exhaust Rakes

Note: Dimensions in mm

FIGURE 2. INLET AND EXHAUST INSTRUMENT RAKES

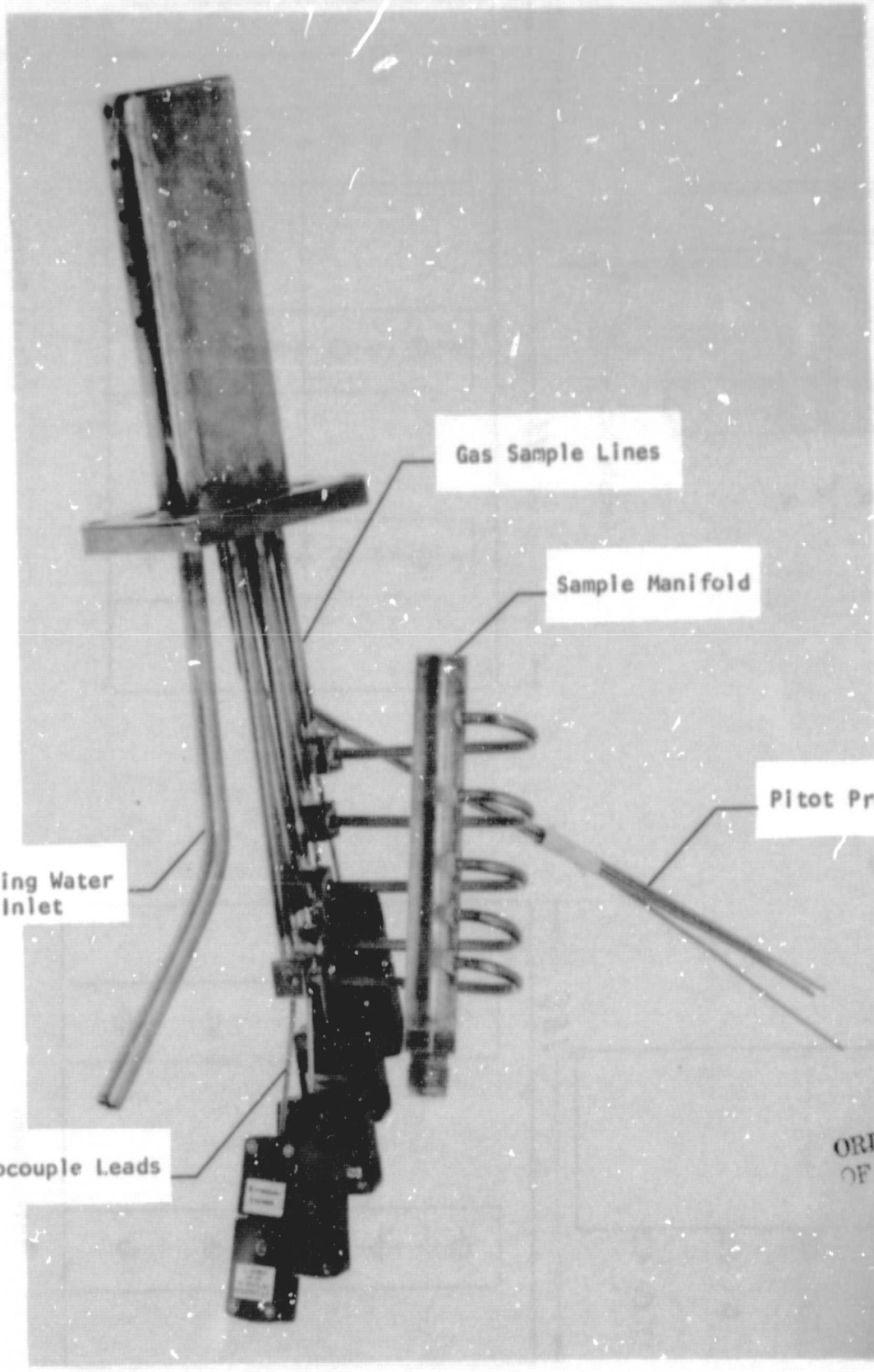

FIGURE 3. PHOTOGRAPH OF WATER-COOLED EXHAUST INSTRUMENTATION RAKE.

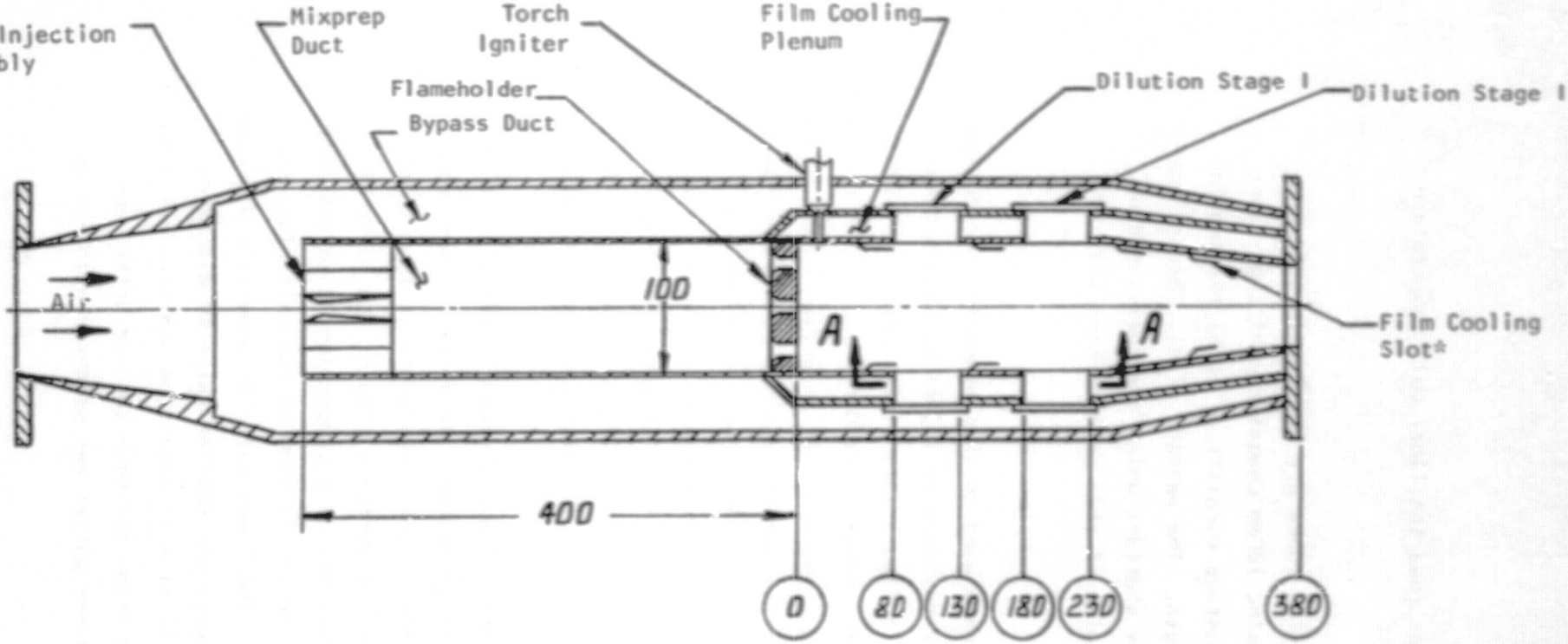

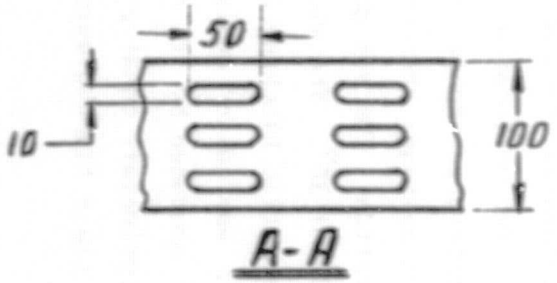

*Slots at stations 80,120,165, 220,260,310 have injection areas representing 25,22,16, 15,13 and 9% of total film cooling, respectively.

FIGURE 4. COMBUSTOR DETAILS

staging configuration. Thermocouples read the liner wall temperature upstream of each film-cooling slot.

Two sets of dilution air injection tubes are provided, the first beginning 80mm and the second beginning 180mm downstream of the flameholder exit station. Each dilution stage consists of three rectangular slots 10mm in width and 50mm in length. The passage of air through the two dilution stages is controlled by shutters which are positioned by externally mounted motors. The details of this construction will be discussed later in this section.

Two fuel injection assemblies were used in this program: one designed to inject liquid Jet-A and the other designed to inject gaseous propane. The two assemblies are illustrated in Figure (5). The propane injection assembly consists of a 12.7mm diameter manifold feeding five 6.35mm diameter injector tubes, each containing five 1.1mm diameter injection holes aligned with the airflow direction. The Jet-A injector consists of a 100mm square array of 25 venturi-shaped modules each of which contains a 1mm dia. injection tube at its throat section which is 6.4mm in diameter. The injector assembly was tested with the fuel injection tubes positioned at the centers of the venturi passages (as shown in Figure 5) and with the injection tubes positioned flush with the walls of the venturi throats.

The perforated plate and vee gutter flameholders are illustrated in Figure (6). The perforated plate design employs an array of 25 holes, 9mm in diameter, to produce a blockage of 84%. The plate is 25mm thick and the hole passages are rounded at the entrance side of the plate to avoid separation. The vee gutter consists of a simple 6mm thick vee with a half-angle of 30°. The width of the vee is 69mm at the exit plane and yields a geometric blockage of 69%. The lower value of geometric blockage used for the vee gutter design reflects the smaller value of discharge coefficient produced by its non-parallel exit condition and the desire to obtain approximately equal pressure drops for both the vee gutter and perforated plate flameholders. The vee gutter was oriented with its axis

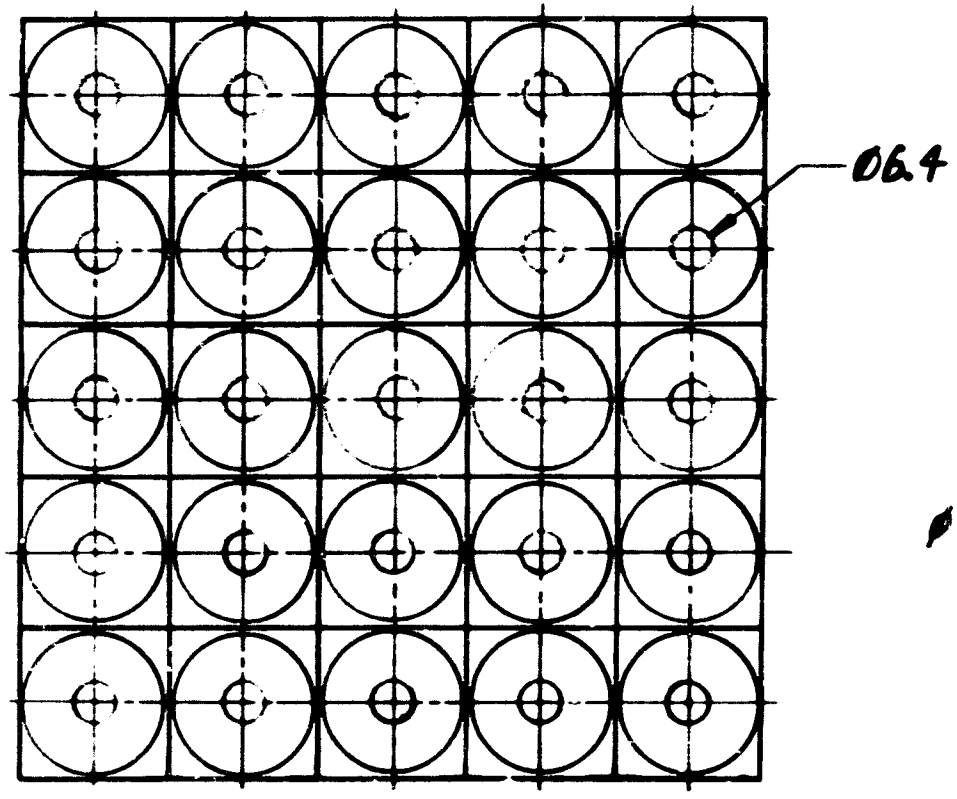

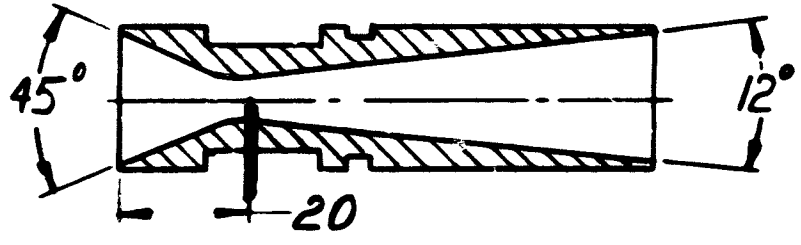

Injector Matrix Element

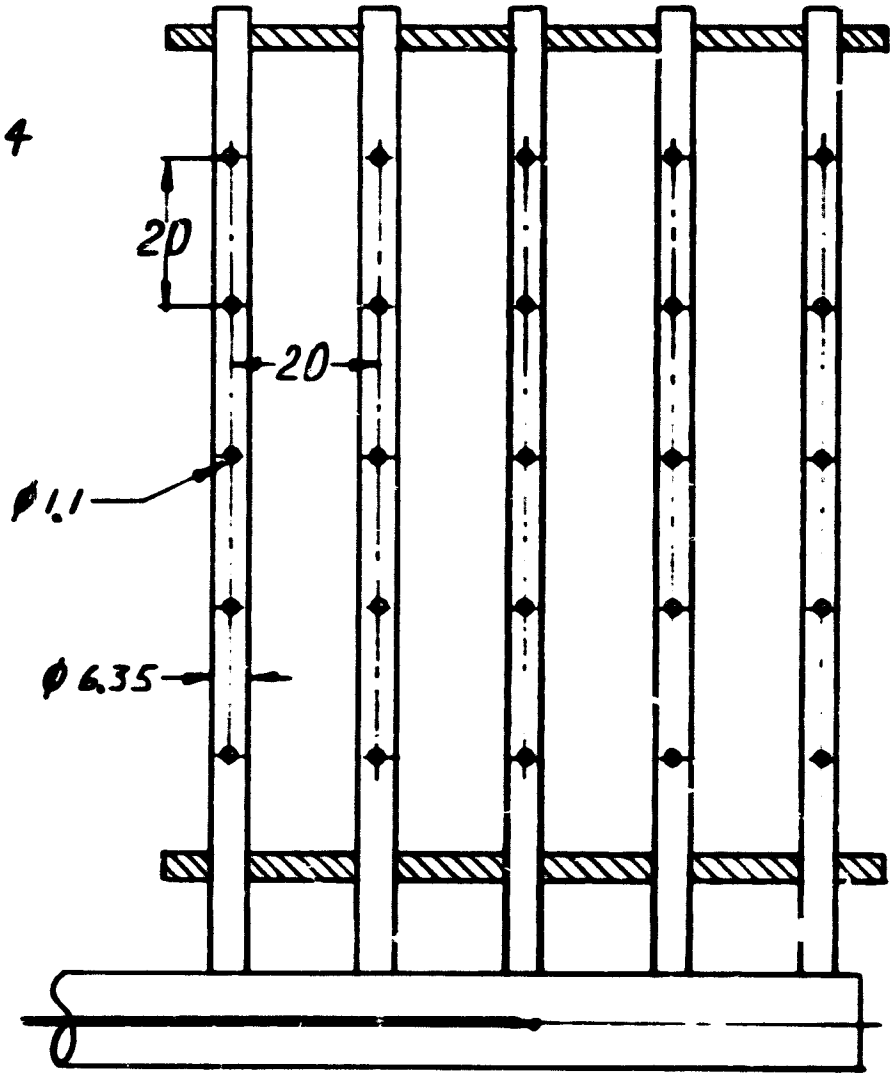

JET-A Injector

Propane Injector

FIGURE 5. DETAILS OF JET-A AND PROPANE FUEL INJECTORS

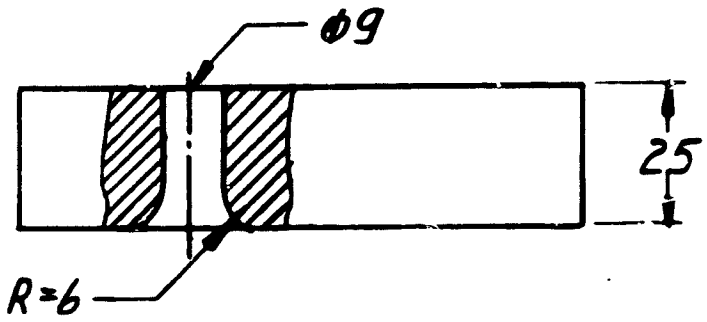

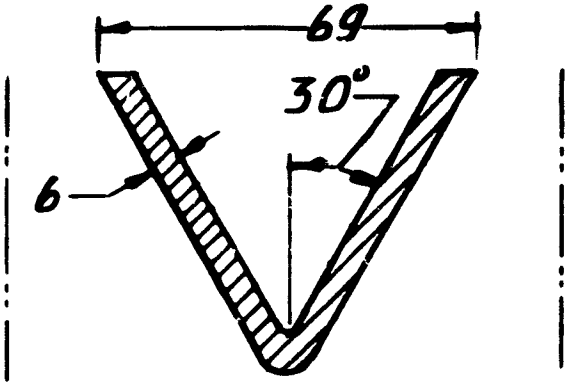

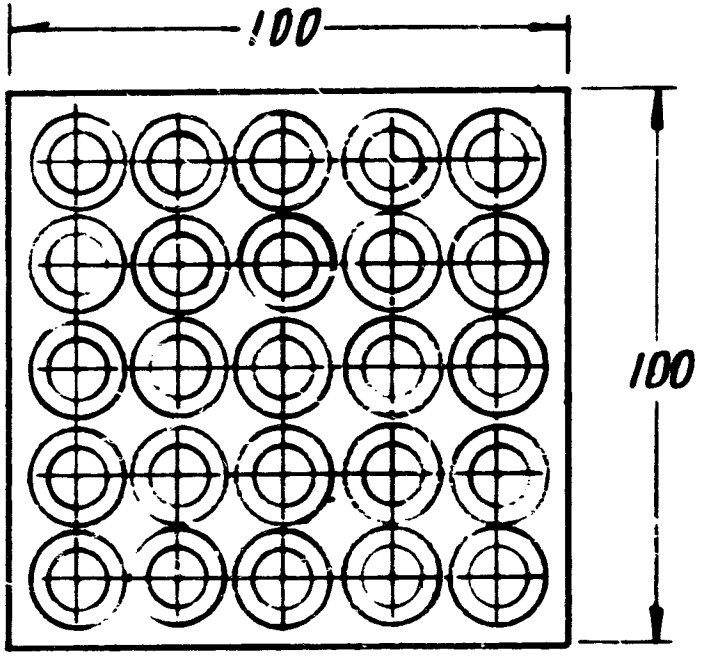

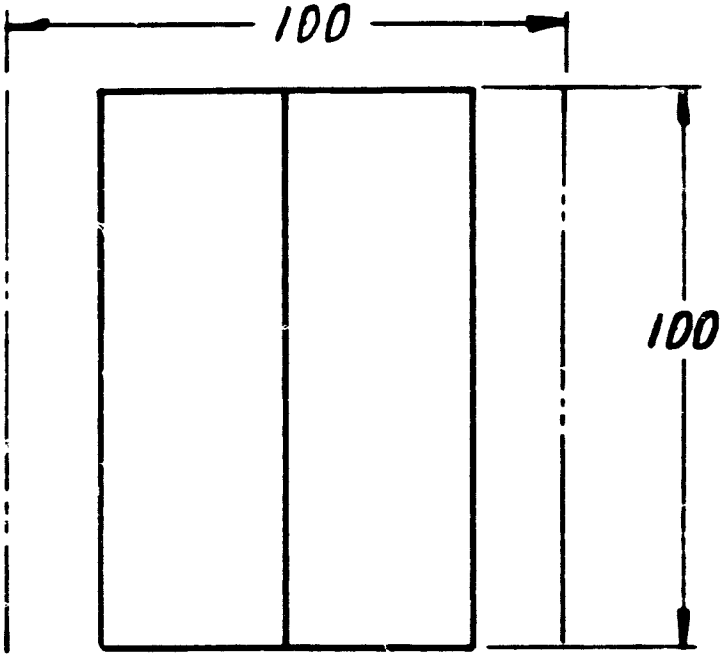

Perforated Plate

Vee Gutter

FIGURE 6. DETAILS OF PERFORATED PLATE AND VEE GUTTER FLAMEHOLDERS

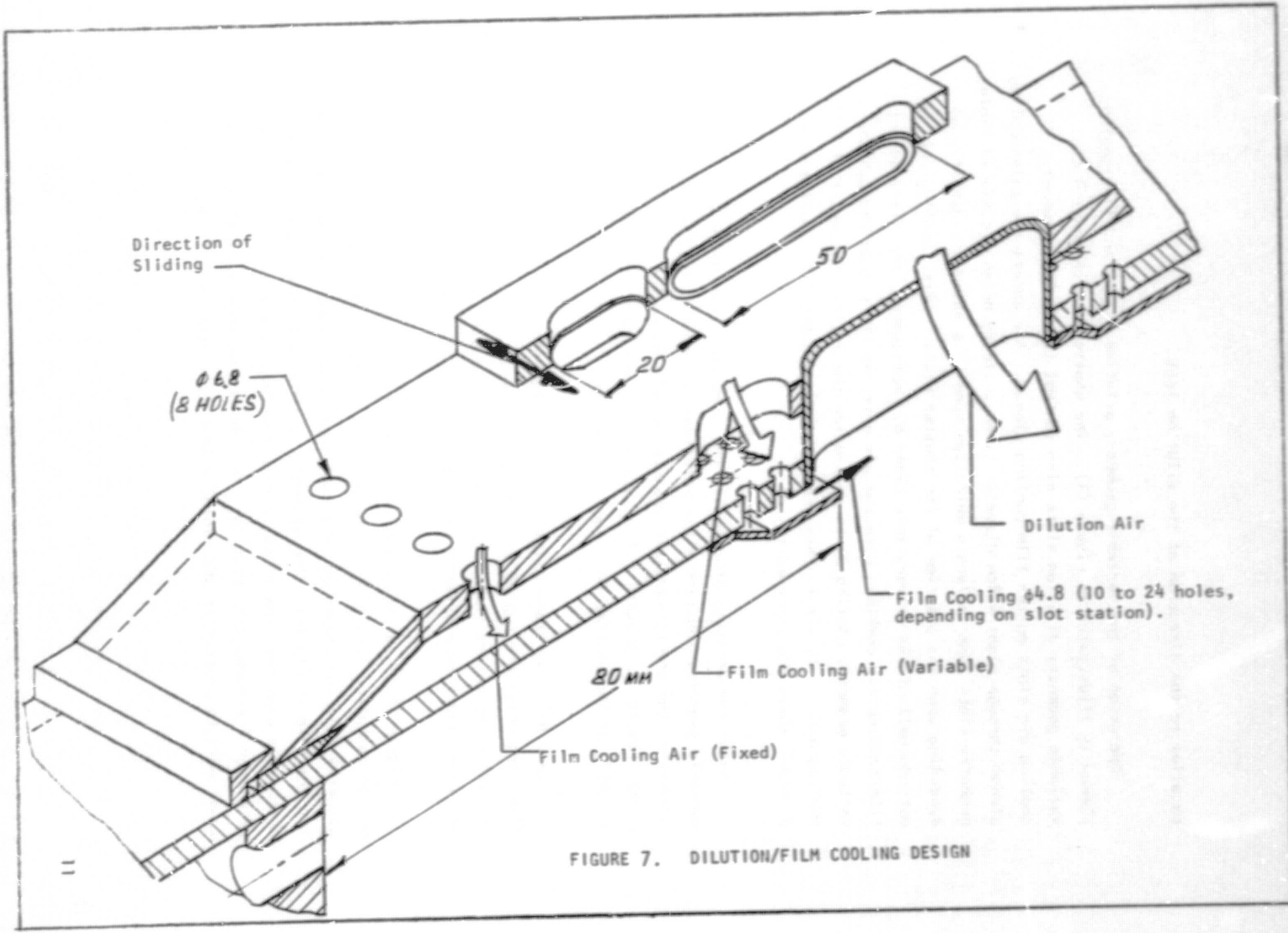

FIGURE 7. DILUTION/FILM COOLING DESIGN

parallel to the direction of the dilution jets.

Operation of the variable geometry dilution stages and film-cooling plenum is illustrated in Figure (7). The shutters which control the variable geometry dilution slots also control the variable geometry cooling air slots on the film-cooling plenum. Air enters the film-cooling plenum through eight 6.8mm diameter fixed geometry holes and six variable geometry slots 20mm in length which can open to a maximum width of 10mm depending upon the position of the shutter plate. After cooling the outside wall of the primary zone liner by impingement, the fixed geometry film-cooling air combines with the air entering the plenum through the variable geometry cooling slots to provide the entire complement of film-cooling air. This air is then exhausted through the film-cooling slots provided along the liner wall.

Since the pressure drop across the combustor liner decreases as the variable geometry shutters allow relatively more dilution air to enter the combustor, the use of variable geometry supply holes for the film-cooling plenum results in a total film-cooling air fraction which varies only slightly as the shutter positions are changed.

Each dilution stage contains three rectangular slots 10mm wide and 50mm long which are opened and closed by movement of the shutter plate. The air which enters these rectangular slots passes through the dilution air tubes and enters directly into the combustion chamber.

Figure (8) is a photograph which illustrates the construction details of the combustor section. The motors which actuate the two variable geometry dilution stages and all instrumentation leads have been removed for the sake of clarity. The assembly is shown with plexiglass sidewalls which were used for flow visualization testing. Stainless steel sidewalls were used for combustion testing. An alumina coating was applied to the inner wall to protect it and minimize heat loss from the system.

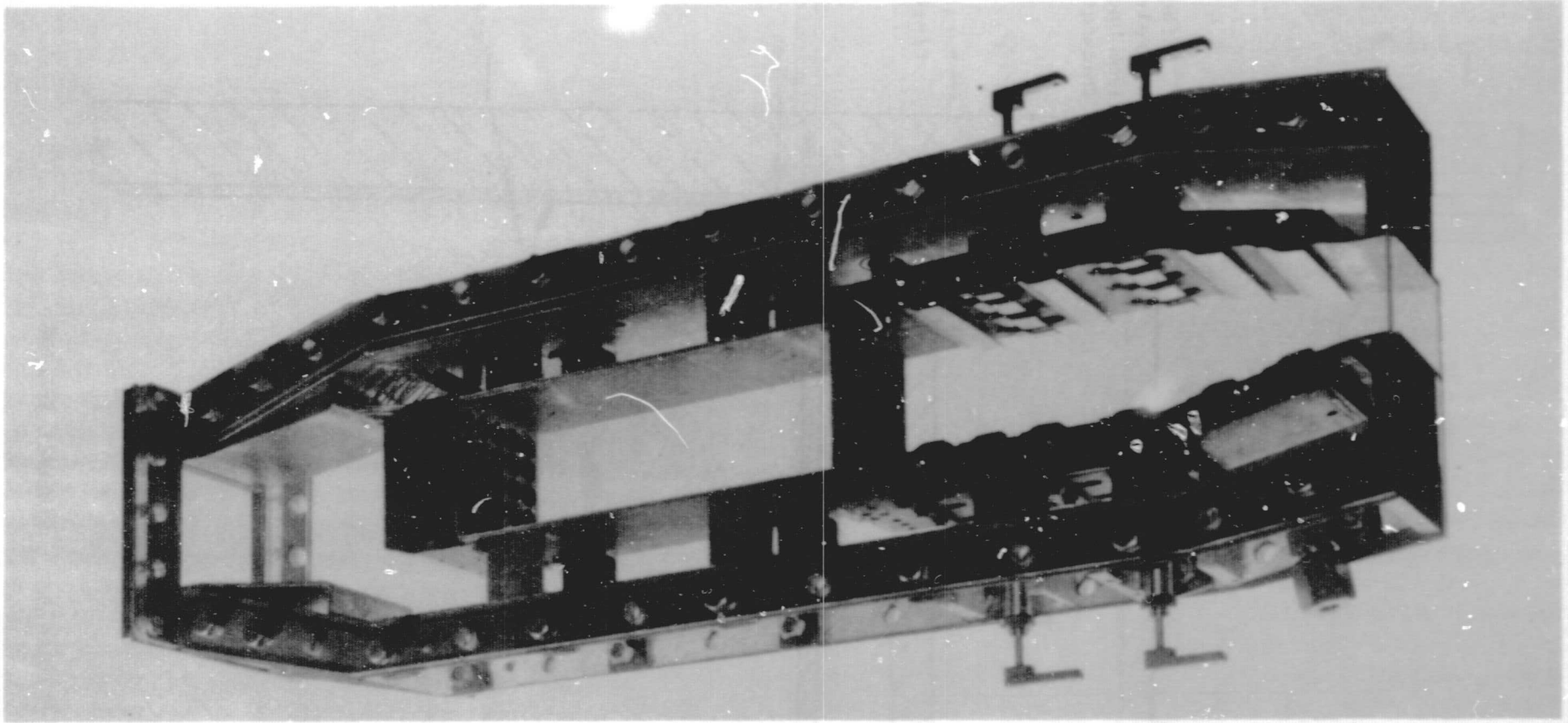

Note: Flameholder shown is not the one used during combusion testing.

FIGURE 8. PHOTOGRAPH SHOWING CONSTRUCTION OF COMBUSTOR SECTION.

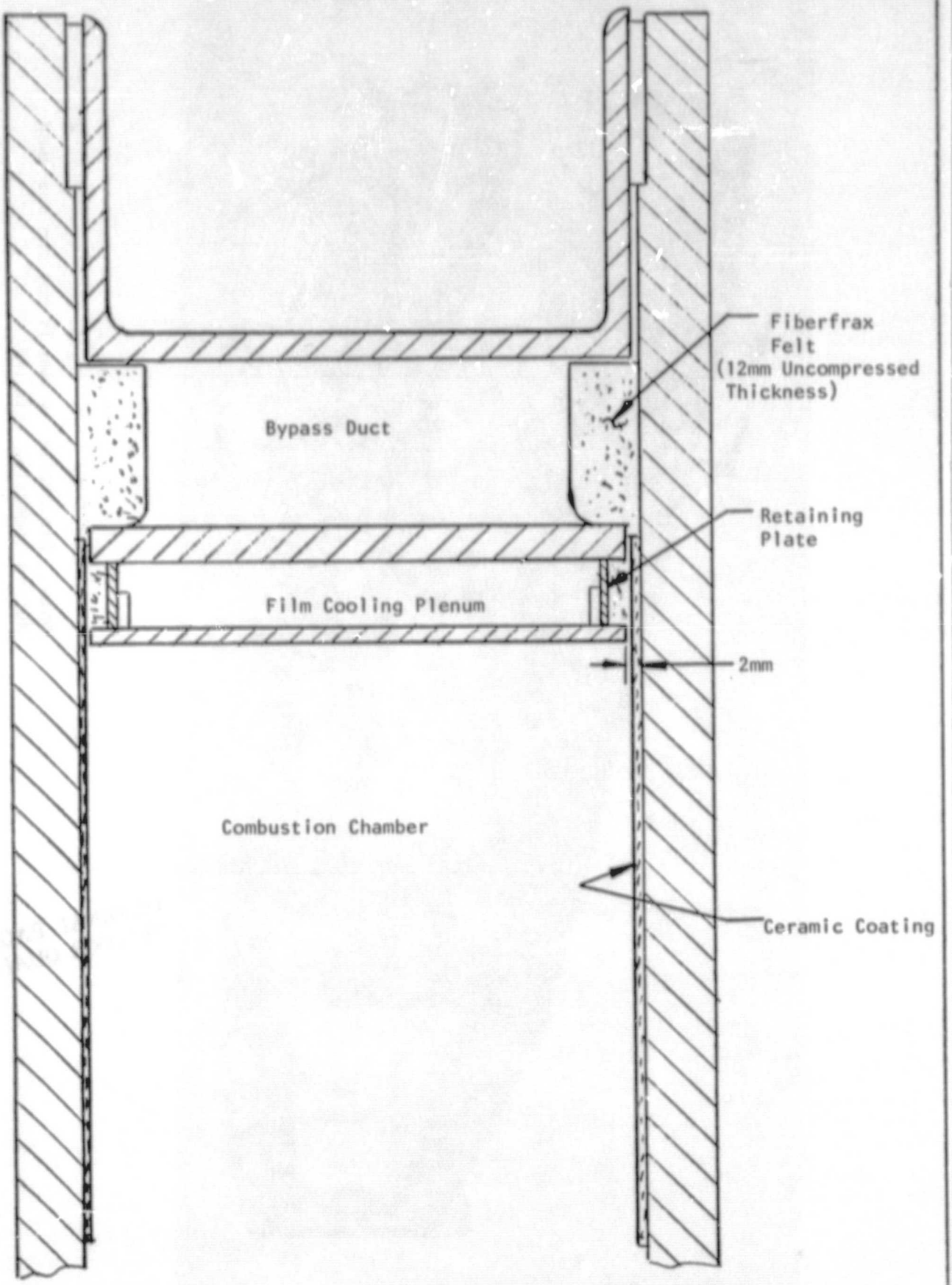

FIGURE 9. SIDEWALL SEALING

The method used to seal the combustor liner to the sidewalls of the test apparatus is illustrated in Figure (9). A number of labyrinth-type seal designs were tested but the leakage rates which these designs produced proved to be more than could be tolerated in the experiment. As a result, the compressed fiberfrax felt design illustrated in Figure (9) was adopted. Here, a strip of ceramic felt material was compressed between the combustor liner assembly and the combustor sidewall while the material was in its soft, uncured condition. Heated air was then passed through the test rig to cure the material, which resulted in a relatively dense ceramic seal at the inner wall of the combustor.

The details of the fuel supply system are illustrated schematically in Figure (10). Liquid fuel is stored in a reservoir which is pressurized using gaseous nitrogen. The fuel is withdrawn near the bottom of the reservoir and passed through a turbine flowmeter, a pressure regulator and cavitating venturi to produce a flow rate determined by the regulator loading pressure and independent of pressure fluctuations in the combustor. The fuel is then passed through a heat exchanger and, finally, through a control valve located next to the test rig. The heat exchanger is not used when firing Jet-A fuel. When firing propane, the exchanger heats the fuel to a temperature of 100^{o}C, slightly above its critical temperature, to assure that only gaseous fuel exits the unit. A thermocouple and pressure tap located in the propane injector supply plenum inside the combustor housing are used to assure that the thermodynamic state of the fuel is such that liquid phase injection is not possible.

Cold flow streamline tracing was carried out using a simple tuft-photo technique. To do this, a plate containing an array of short wool tufts was mounted 4mm off the center plane of the combustor. The tufts were mounted to the plate such that they extended approximately 4mm from the plate surface before aligning themselves with the local airflow direction, thereby positioning themselves in the center plane of the flowfield away from the plate boundary layer. The tuft pattern produced by each geometric configuration of interest was photographed and yielded a result similar to

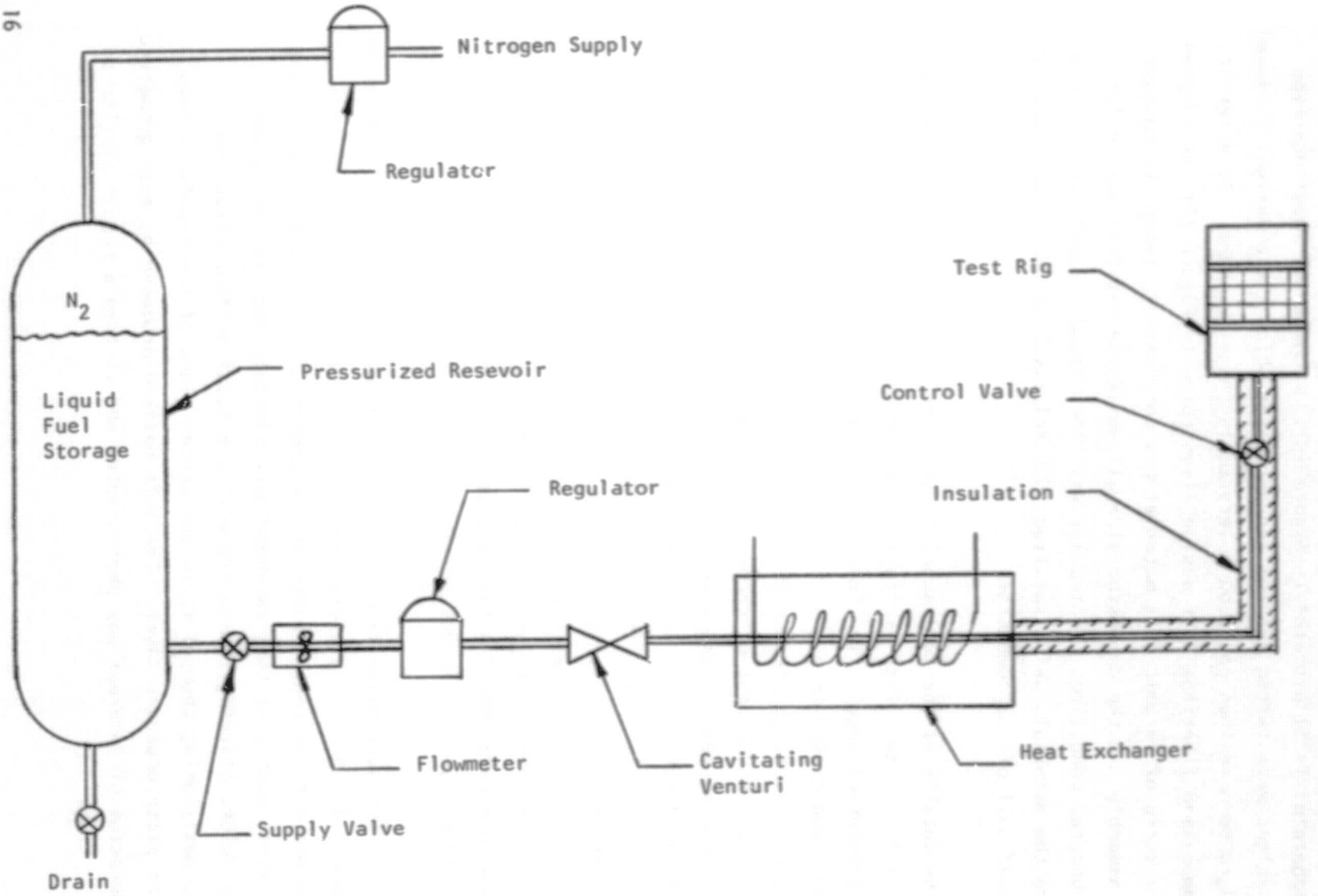

FIGURE 10. FUEL SYSTEM DETAILS

FIGURE 11. METHOD OF STREAMLINE TRACING FROM WOOL TUFT PHOTO

that illustrated in Figure (11). Streamlines were traced through the flowfield by starting at arbitrary points downstream of the flameholder and requiring that the local streamline slope match the local (interpolated) tuft slope at all points. Tuft photography and streamline tracing were carried out for each flameholder at six combinations of dilution staging configuration. Designating the dilution staging configurations by the percent opening of the first/second stage shutters, streamlines were traced at the following conditions: 50/0; 0/50; 100/0; 50/50; 100/100.

Although tuft photography is a simple and reliable method of streamline tracing, it suffers from the disadvantage of being geometrically coarse due to the necessity of spacing the tufts far enough from one another to prevent interaction. This limitation prevents the technique from yielding accurate information about the size of the recirculation region attached to the perforated plate flameholder. (The vee gutter recirculation zone is large enough to be well-defined by the tuft photos.) Therefore, the recirculation zone produced by the perforated plate was made visible by placing an oil-coated plate directly on the centerplane of the combustor and observing the resulting oil flow pattern. Although this technique involves some interaction with the oil-plate boundary layer, the fact that its use was restricted to a region less than 80mm from the plate leading edge makes the degree of error acceptably small.

A tracer gas technique at ambient entrance conditions was used to look into secondary air entrainment in the recirculation zones of the two flameholders. The technique is illustrated schematically in Figure (12). Carbon monoxide is injected into the primary air through the fuel injection assembly to produce a uniform dispersion of the gas in the mixprep duct. A sample of the primary gas is withdrawn just upstream of the flameholder recirculation zone as shown in the figure. The ratio of CO concentration in the flameholder recirculation zone to that in the primary air is assumed to be a reasonable approximation to the ratio of fuel concentrations (equivalence ratios) in these two regions during combustor operation.

Both the tracer gas and the flow visualization tests were carried out

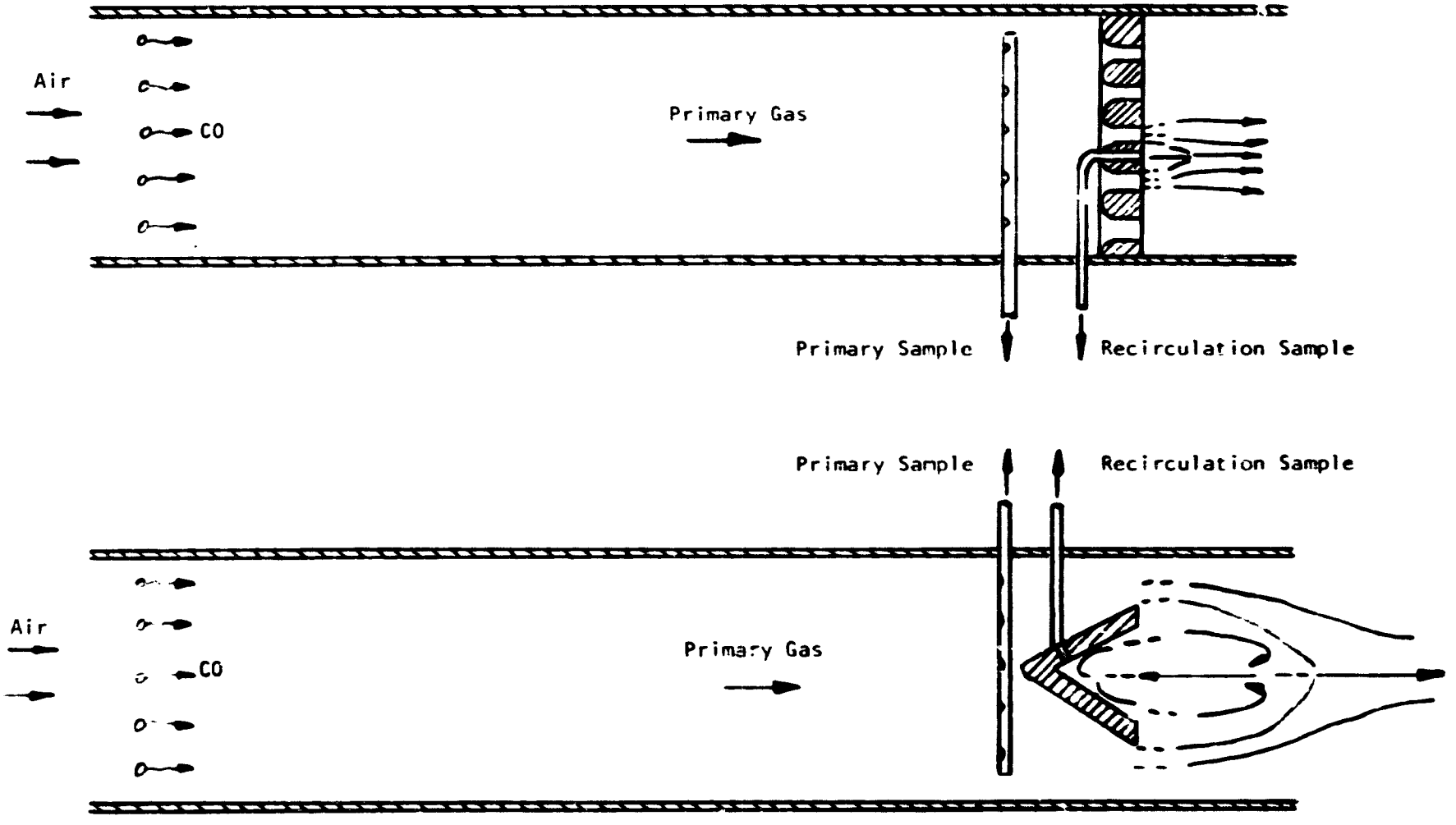

FIGURE 12. TRACER GAS SAMPLING TECHNIQUE

at a reference velocity of 30 m/s with nominally ambient inlet pressure and temperature. The Reynolds number for these tests, based on reference velocity and combustor height, was 6.8×10^4, which compares favorably with the reference Reynolds number of 11×10^4 during combustion testing.

Combustion testing was carried out at inlet conditions of 5 atm/630K and a reference velocity of 30 m/s. The test procedure consisted of setting the dilution zone shutters in the position desired, bringing the airflow up to the proper level, igniting and increasing primary zone equivalence ratio to approximately 0.5, turning off the gas igniter, adjusting operating pressure and then recording data. The fuel flow rate was then increased until one of the following conditions occurred: overall equivalence ratio reached 0.6, primary zone equivalence ratio reached 1.1, liner wall temperature exceeded 1200K, flashback occurred. The purpose behind limiting primary zone equivalence ratio will be discussed shortly. The fuel flow rate was then reduced, in steps, until the lean stability limit was reached.

During combustion testing, a gas sample was withdrawn from the mixprep section using the primary sample rake used in earlier tracer gas testing. This sample was passed through a catalytic reactor and then analyzed for CO_2 content to determine primary zone equivalence ratio. This measurement served two purposes. First, it provided a means of determining combustor primary/secondary airflow split independent of calculations based on open areas and discharge coefficients. Second, it provided a mechanism to monitor primary zone equivalence ratio during testing. It was noted earlier that one of the criteria for limiting fuel flow rate was that of primary zone equivalence ratio reaching 1.1. This limitation is a corollary of the liner wall temperature limit, since the addition of film-cooling air to a hot fuel-rich stream produces flames at the cooling slots and causes liner damage. The placement of the wall temperature thermocouples was such that flames at the film cooling slots could not be sensed quickly enough, so the rich primary zone exclusion was added to the list of operating restrictions.

The gas analysis system used in these tests was in conformance with SAE ARP 1256 and is described in the Appendix.

RESULTS

This section presents the combustor streamline patterns and tracer gas test results, followed by a presentation of flashback and lean stability limits and emissions characteristics for both flameholder configurations.

Streamline Patterns

Figure (13) presents the results of the flow visualization tests for the perforated plate flameholder. As a general comment, the recirculation zone attached to the perforated plate increases in streamwise extent near the liner wall. For the six dilution staging configurations tested, the flameholder recirculation zone never extends sufficiently far downstream to merge with the air jets entering from the first dilution stage. The length of the flameholder recirculation zone decreases as the amount of dilution air added to the combustor increases, reflecting the lower combustor entrance plane velocity which prevails under these conditions.

From Figure (13a) (shutter position50/0)*, the first stage dilution jets are seen to be capable of penetrating to the combustor centerline within an axial distance of approximately 80mm. It should be noted that the seeming violation of flow continuity which is evidenced by the fact that the dilution jets approach the combustor centerline is a result of the three-dimensional nature of the combustor flow field. Since dilution air is added through three distinct rectangular slots in each stage, the introduction of this air causes the combustor mainstream to turn out of the plane of the figure and flow around the obstructions represented by the dilution jets. As a result, there is loss of mainstream flow in the streamline plane represented here. Figure (13b) shows that increasing the open area of the first dilution stage (shutter position 100/0) increases the mass of dilution air added to the combustor but decreases the penetration of the dilution jets due to the lower pressure drop and correspondingly lower entrance velocity produced by this configuration. Figure (13c)

---

*Dilution staging configurations are designated in the form A/B where A and B are the open areas of the first and second dilution stages, respectively, in percent.

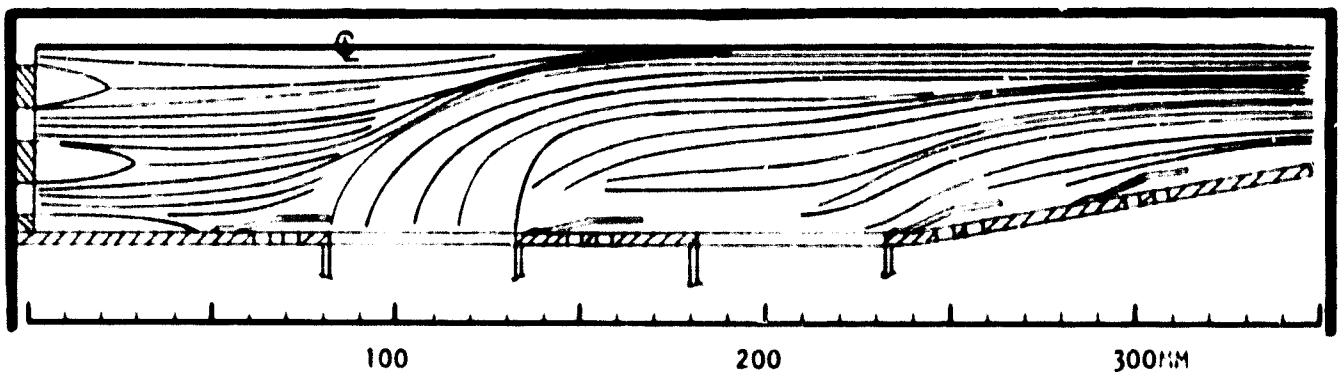

a. STAGE I 50% OPEN - STAGE II CLOSED

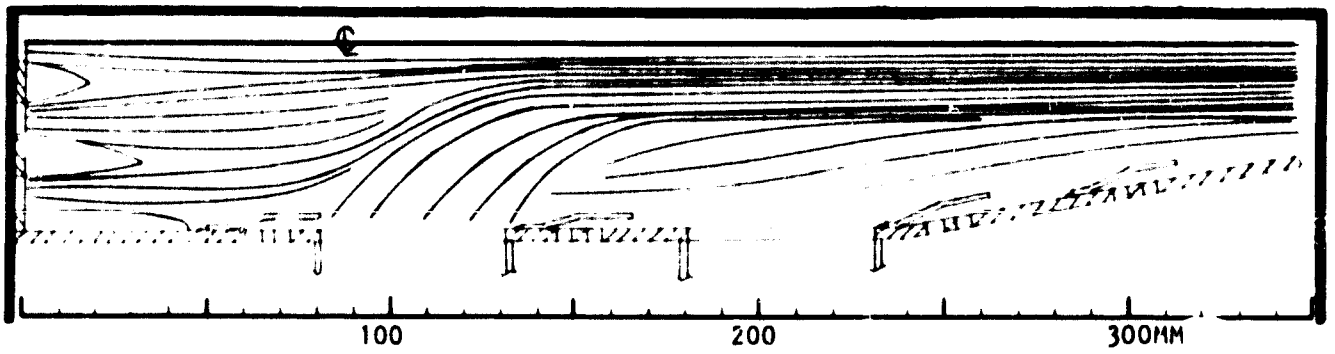

b. STAGE I 100% OPEN - STAGE II CLOSED

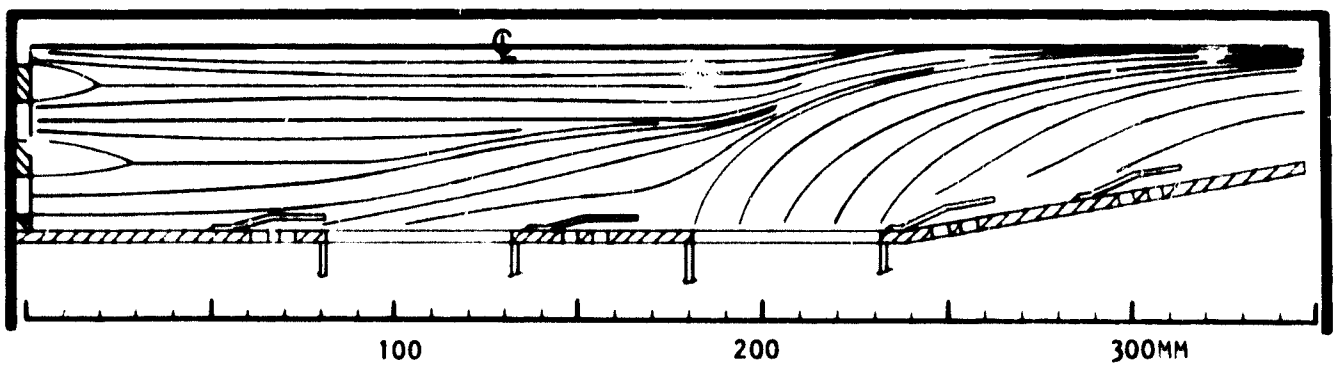

c. STAGE I CLOSED - STAGE II 50% OPEN

FIGURE 13. CENTERPLANE STREAMLINE PATTERN FOR PERFORATED PLATE FLAMEHOLDER.

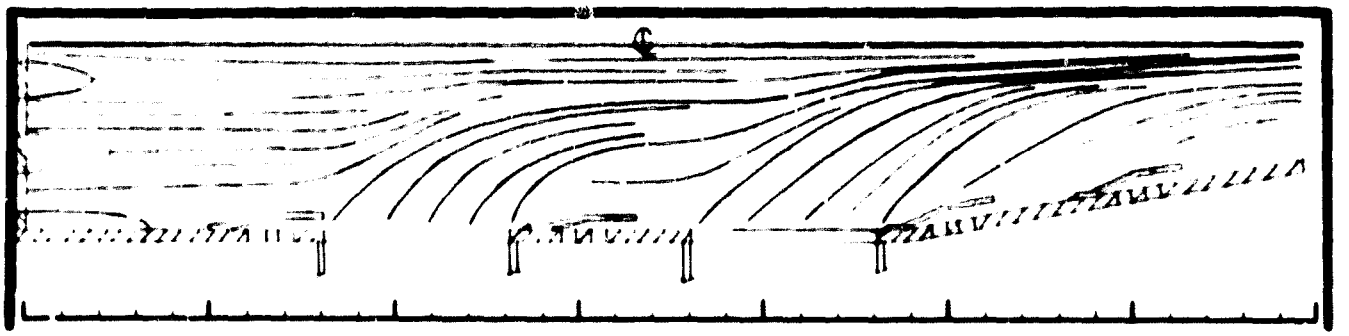

d. STAGE I 50% OPEN - STAGE II 50% OPEN

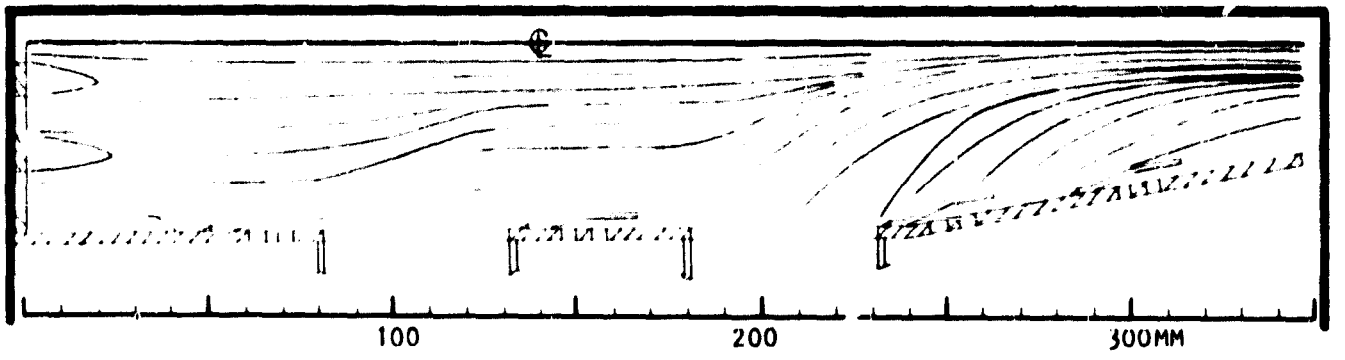

e. STAGE I CLOSED - STAGE II 100% OPEN

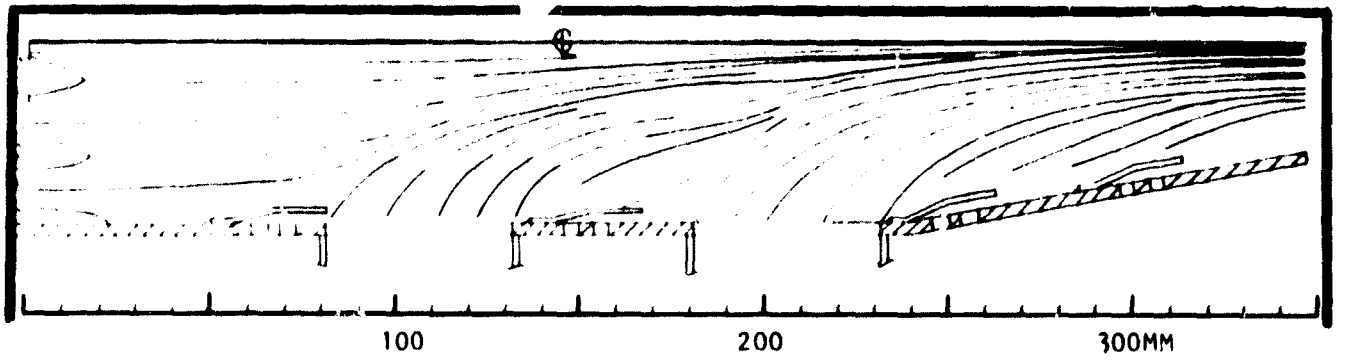

f. STAGE I 100% OPEN - STAGE II 100% OPEN

FIGURE 13 (CONT'D.) CENTERPLANE STREAMLINE PATTERN FOR PERFORATED PLATE FLAMEHOLDER.

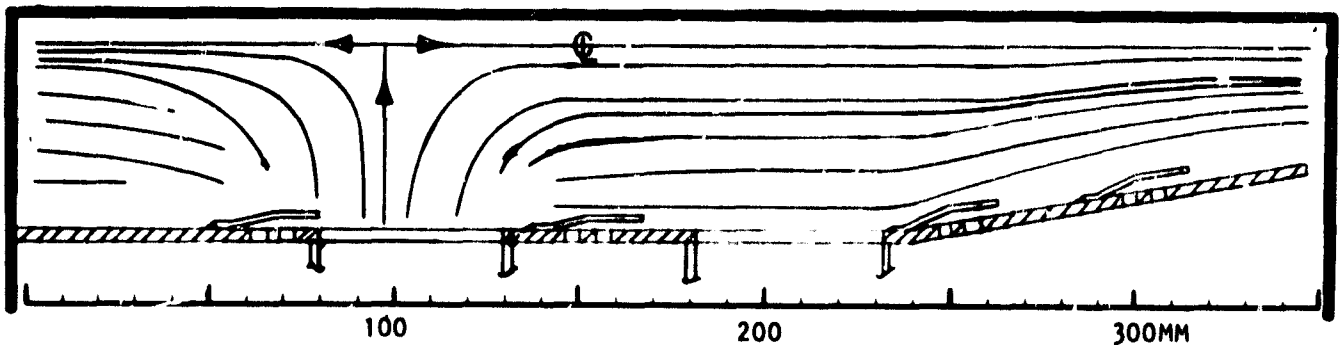

a. STAGE I 50% OPEN - STAGE II CLOSED

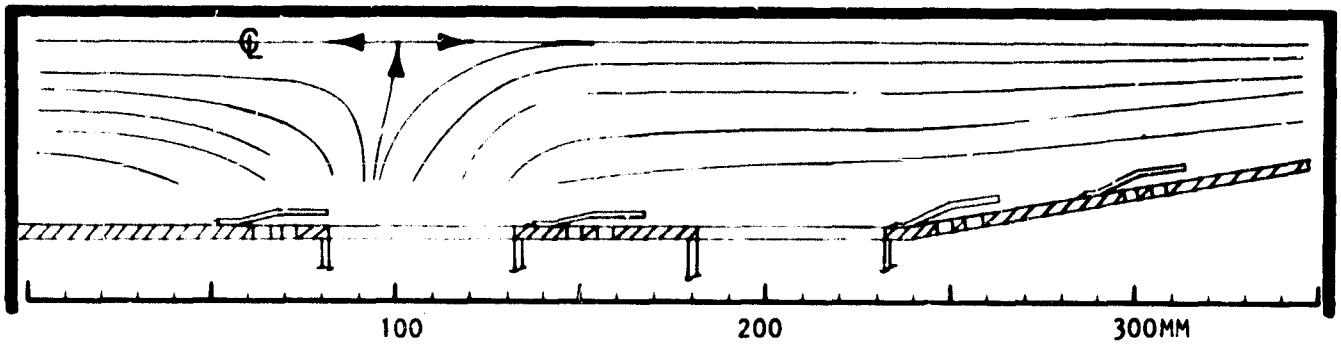

b. STAGE I 100% OPEN - STAGE II CLOSED

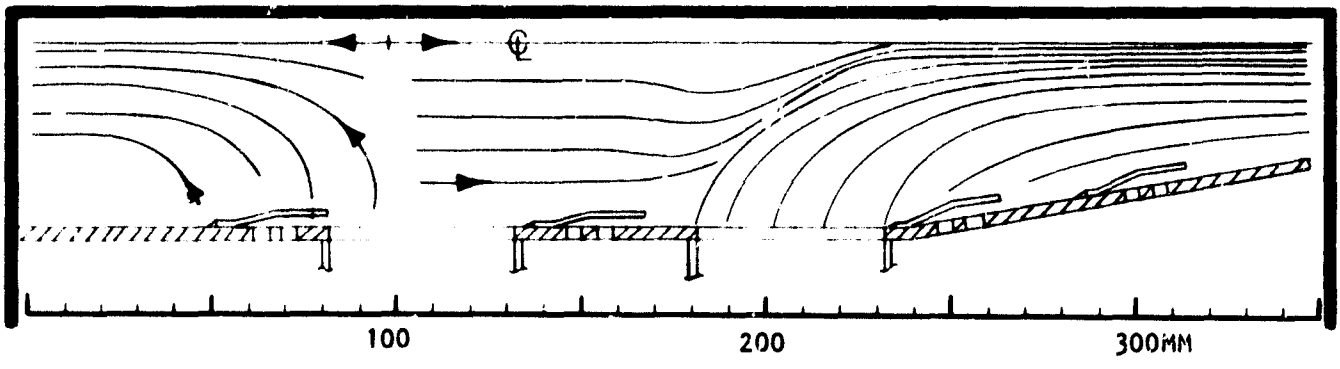

c. STAGE I CLOSED - STAGE II 50% OPEN

FIGURE 14. CENTERPLANE STREAMLINE PATTERN FOR VEE GUTTER FLAMEHOLDER.

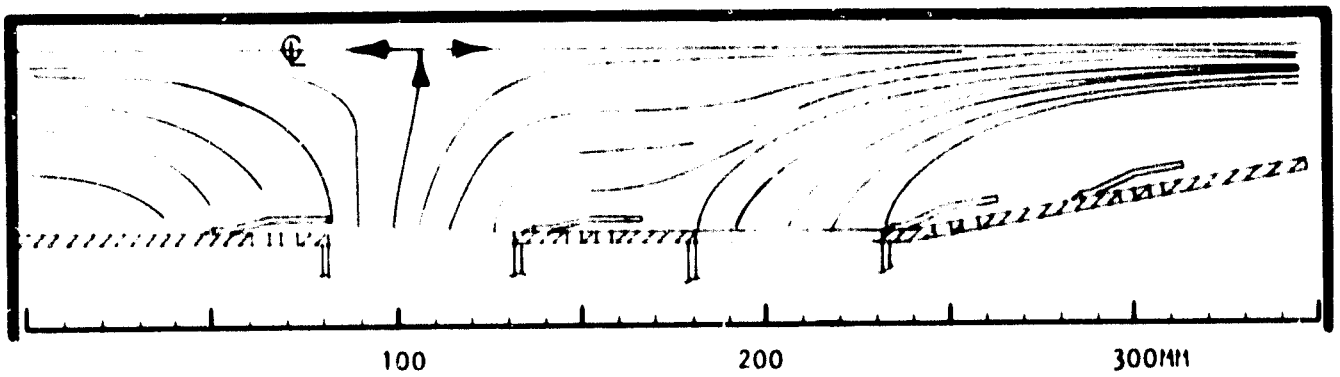

d. STAGE I 50% OPEN - STAGE II 50% OPEN

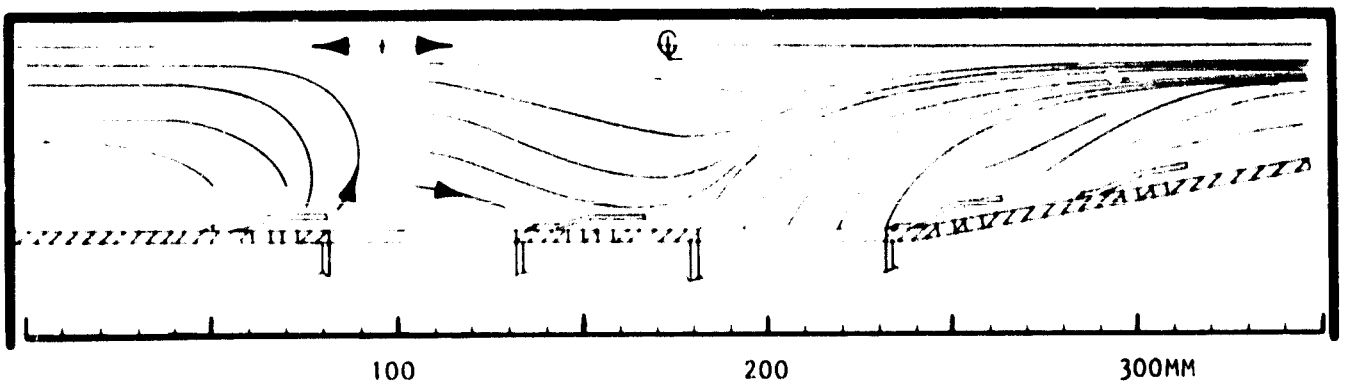

e. STAGE I CLOSED - STAGE II 100% OPEN

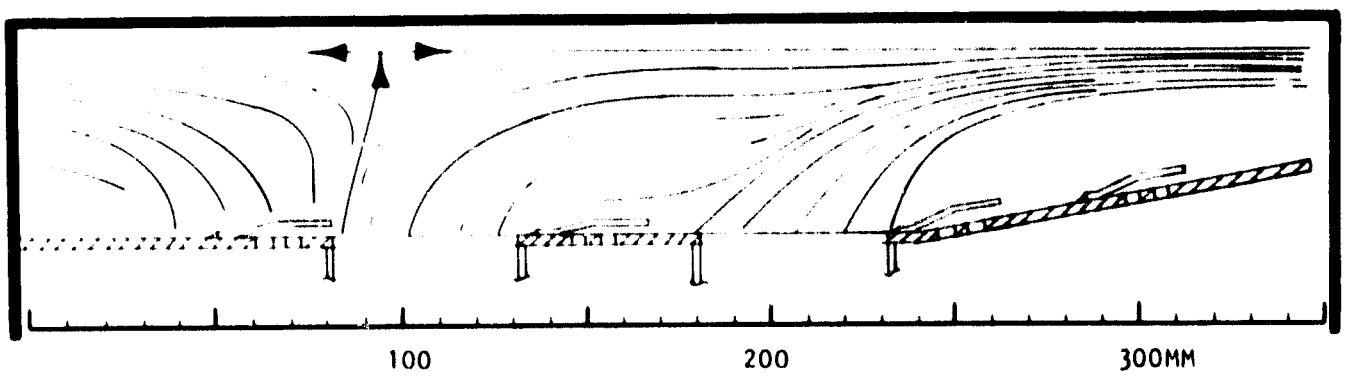

f. STAGE I 100% OPEN - STAGE II 100% OPEN

FIGURE 14 (CONT'D.) CENTERPLANE STREAMLINE PATTERN FOR VEE GUTTER FLAMEHOLDER.

indicates that the same rapid penetration is achieved when dilution air is added through the second stage (shutter position 0/50) as occurs when the first stage is employed. Figure (13d) illustrates that adding dilution air equally through each of the two dilution stages (shutter position 50/50) results in an initial decrease in penetration of the first stage jet (the total pressure drop of this configuration is the same as that of the low penetration 100/0 configuration illustrated in Figure (13b)) but the action of the second dilution jet is such that the first jet is eventually pushed upward, reaching the combustor centerline. Figure (13e) illustrates that the same loss of jet penetration is experienced when dilution air is added in the second stage (shutter position 0/100) as when the dilution air is added only in the first stage. Finally, Figure (13f) indicates that even the lowest combustor entrance velocity condition (shutter position 100/100) is capable of producing eventual jet penetration to the centerline due to the additive effects of the first and second stages.

Figure (14) presents the streamline patterns obtained using the vee gutter flameholder. As a general statement, it can be observed that increasing the total area available for dilution air to enter the combustor causes the rear stagnation point of the vee gutter wake to move closer to the flameholder exit plane. Figure (14a) (shutter position 50/0) shows a flow pattern considerably different from that obtained with the perforated plate flameholder with a stagnation point occurring about 100mm downstream of the flameholder exit plane. The large downstream extent of the flameholder near wake results in entrainment of portions of the first dilution jet and air exiting the first film-cooling slot. An interesting result of this entrainment is the ability of the dilution jet to penetrate entirely to the combustor centerline. Increasing the opening of the first dilution stage (shutter position 100/0) is seen to produce only a small variation in behavior, as illustrated in Figure (14b), where the jet can be seen to turn downstream somewhat faster. Figure (14c) illustrates the streamline pattern obtained with the first dilution stage fully closed and the second stage open 50%. Interestingly, there is still a substantial component of velocity at the first dilution stage in the direction of the combustor

centerline. This results from the entrainment of air entering the combustor through the first film-cooling slot. The penetration of the dilution air jet from the second stage slot appears to be nearly identical to that observed at the same shutter position with the perforated plate flameholder. Figure (14d) illustrates the symmetric injection streamline pattern (shutter position 50/50). Here, the penetration of the first dilution jet is nearly identical to that observed for dilution through the first stage only while the penetration of the second stage dilution jet is essentially the same as that observed for the perforated plate flameholder. The streamline pattern obtained with the first dilution stage closed and the second stage fully open is shown in Figure (14c). Here there is an interesting change in the details of the flow between the first and second dilution stages where an ejector-like effect of the second dilution jet causes the primary zone gas stream to be turned away from the combustor centerline. Again, there is evidence of significant entrainment of the air exiting the first film-cooling slot with a significant component of velocity in the direction of the combustor centerline. Figure (14f) illustrates the streamline pattern obtained with both dilution stages fully open. Again, there is complete penetration of the first stage dilution jet although the lower jet velocity at this low pressure drop condition allows much of the air to be turned quickly downstream. The penetration of the second stage jet is again complete.

Tracer Gas Results

The measured values of fuel concentration in the flameholder recirculation zones are presented in Figure 15 and 16 as percentages of fuel concentration in the entering primary gas stream. When the dilution shutters are in the closed position (secondary air consists entirely of film cooling air), both flameholders experience their maximum degree of secondary air entrainment with the perforated plate experiencing nearly 30% dilution and the vee gutter nearly 60% dilution. Dilution of the flameholder recirculation zones appears to be independent of the specific details of dilution staging and is a function only of the amount of air bypassed with the high pressure drop high entrance velocity configurations experiencing the higher degrees

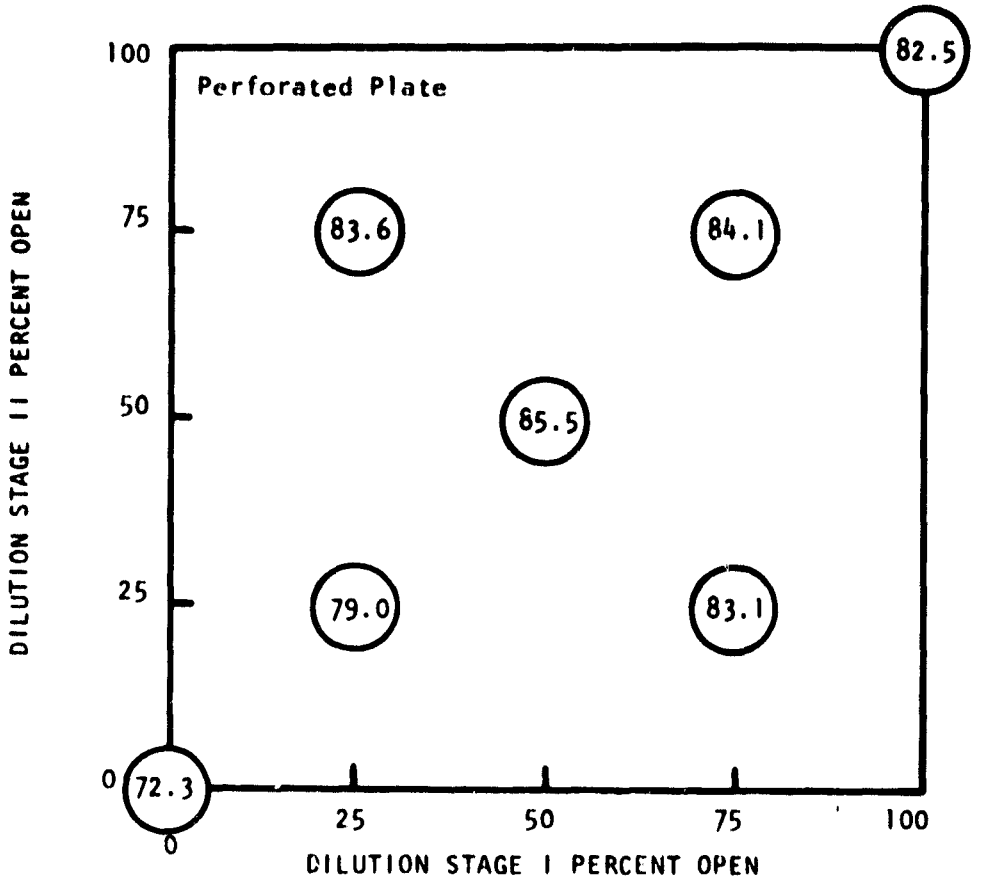

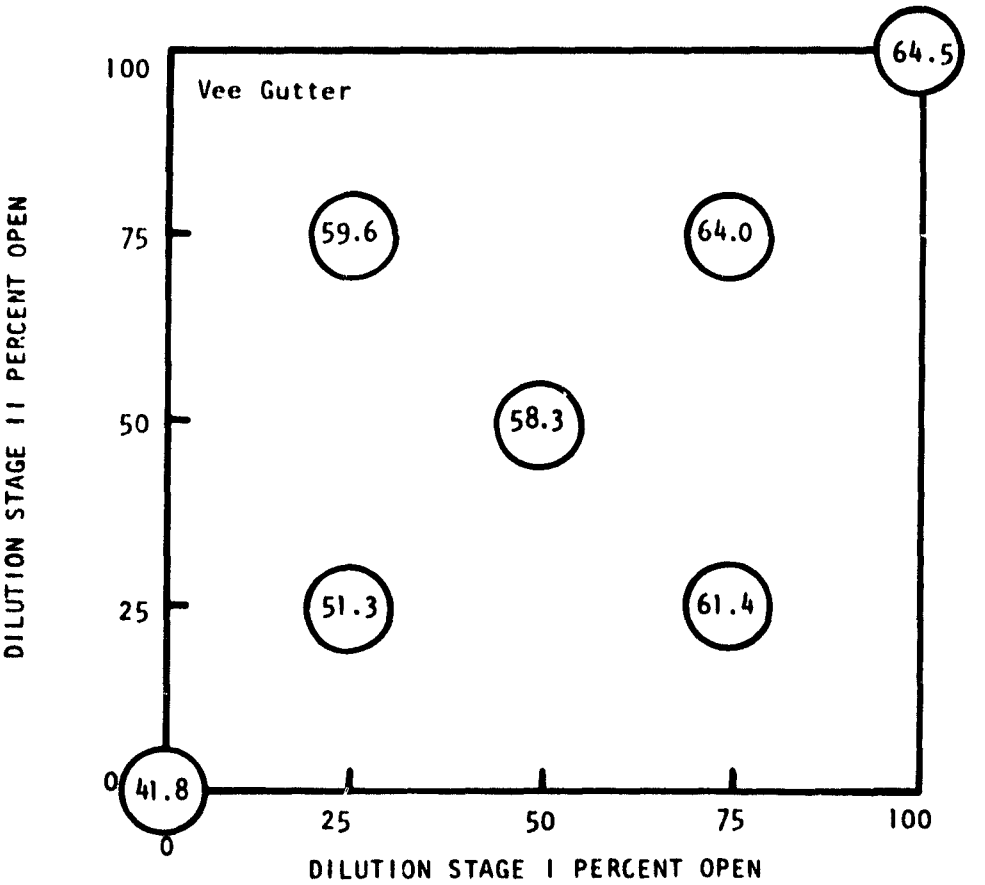

FIGURE 15. PERCENT PRIMARY ZONE FUEL CONCENTRATION IN FLAMEHOLDER RECIRCULATION ZONES.

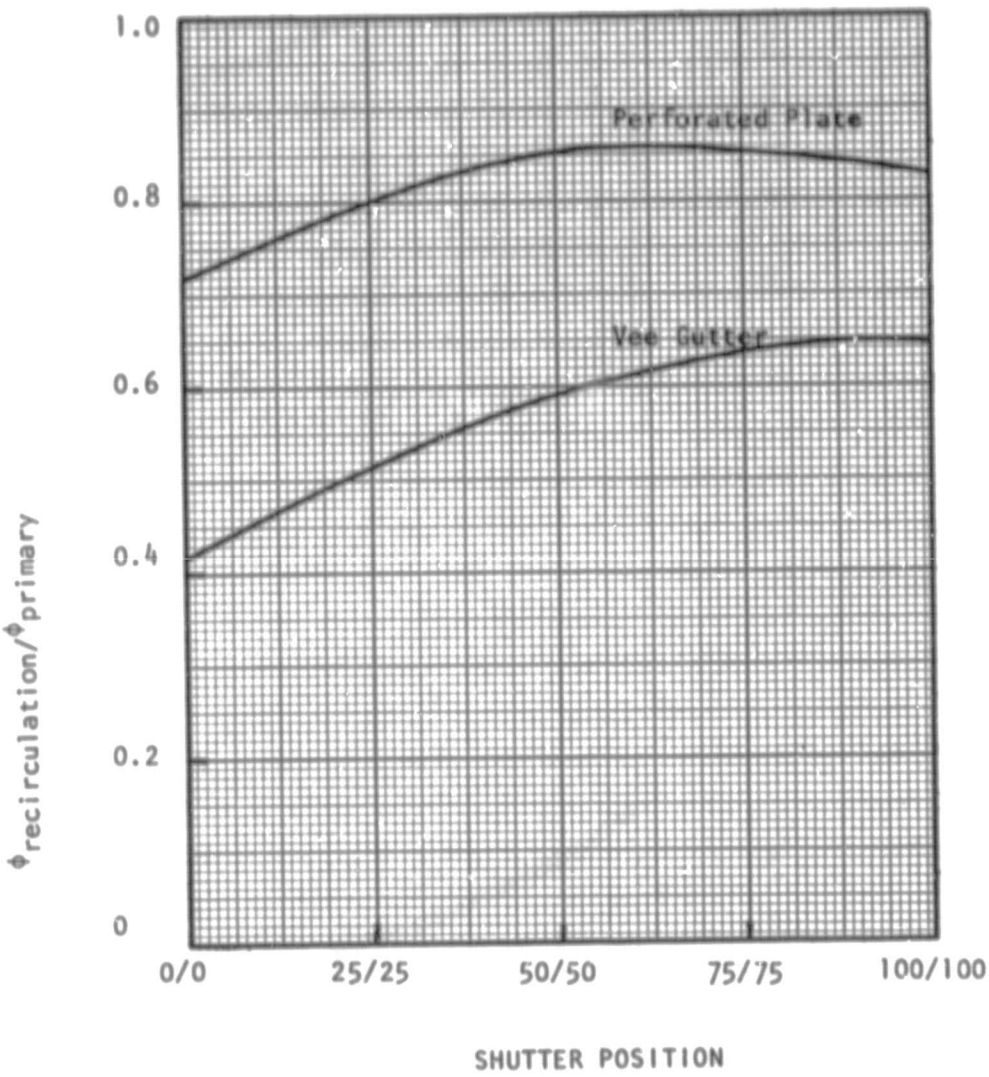

FIGURE 16. FRACTION OF PRIMARY ZONE CONCENTRATION IN FLAMEHOLDER RECIRCULATION ZONES.

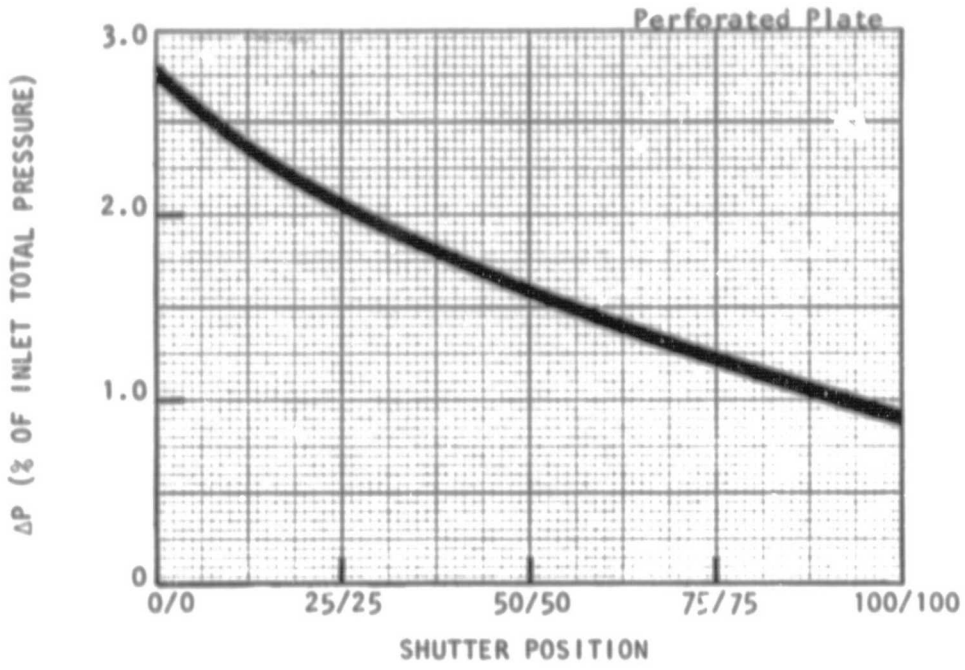

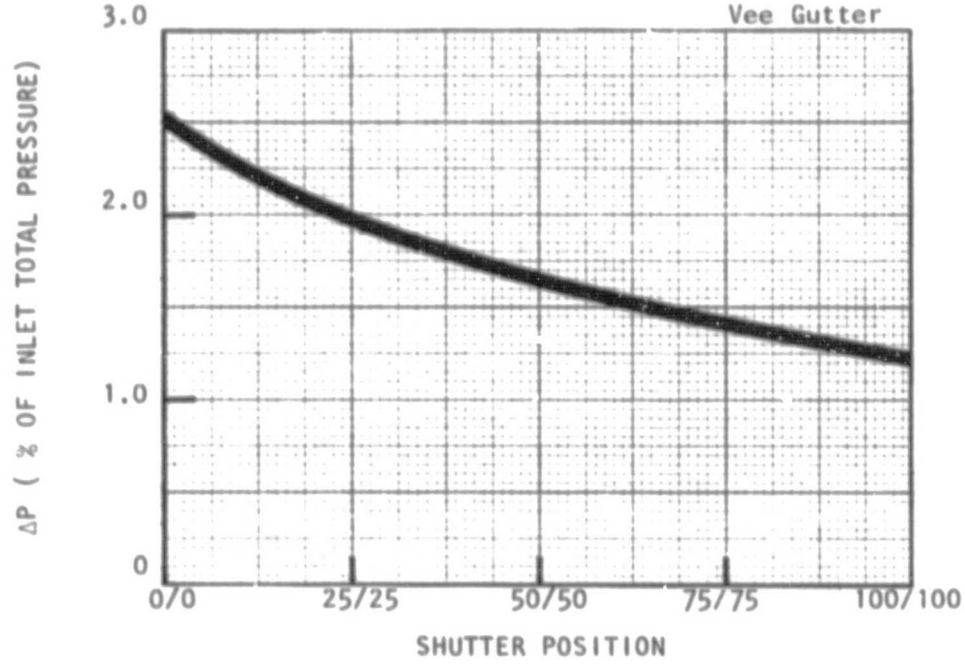

FIGURE 17. PRESSURE DROP CHARACTERISTICS FOR THE PERFORATED PLATE AND VEE GUTTER FLAMEHOLDERS

of dilution.

Combustion Testing - Propane

Combustor Pressure Drop - The combustor pressure drop produced by the perforated plate and vee gutter configurations is presented in Figure (17). The perforated plate produced a slightly higher maximum pressure drop than the vee gutter (2.75% as opposed to 2.5%) and a slightly lower minimum value (0.9% as compared with 1.2%) but these differences are relatively minor and the pressure drop/combustor geometry characteristics of the two configurations can be considered essentially the same. In all cases, combustor pressure drop varied slightly with operating equivalence ratio. The magnitude of this variation is represented in the figure by the width of the curve.

Flow Split - Figure (18) shows the primary/secondary airflow split as a function of dilution staging for the perforated plate and vee gutter flameholders. The film-cooling airflow varies from 18% to 24% of the total combustor airflow for the perforated plate design and from 13% to 22% for the vee gutter. The amount of dilution air admitted by the dilution shutters reaches a maximum of 50% of the total combustor airflow for the perforated plate flameholder and 45% of the total combustor airflow for the vee gutter. Although the figure presents airflow splits for symmetric dilution staging configurations, it was found that flow split is a function of total dilution entrance area only. As a result, the flow split for asymmetric dilution zone geometries such as 25/75 or 75/25 would be the same as that for the symmetric geometry 50/50, since the total open area in the three cases is the same. The flow splits are summarized in Table I.

Stability - Figure (19) illustrates the range of stable operation using the perforated plate flameholder. Combustor entrance velocity is defined here as gas velocity at the exit plane of the flameholder and varies as the total dilution entrance area is varied. The open data points along each constant combustor entrance velocity line indicate measured points of stable operation. The solid data symbols in the figure indicate the values

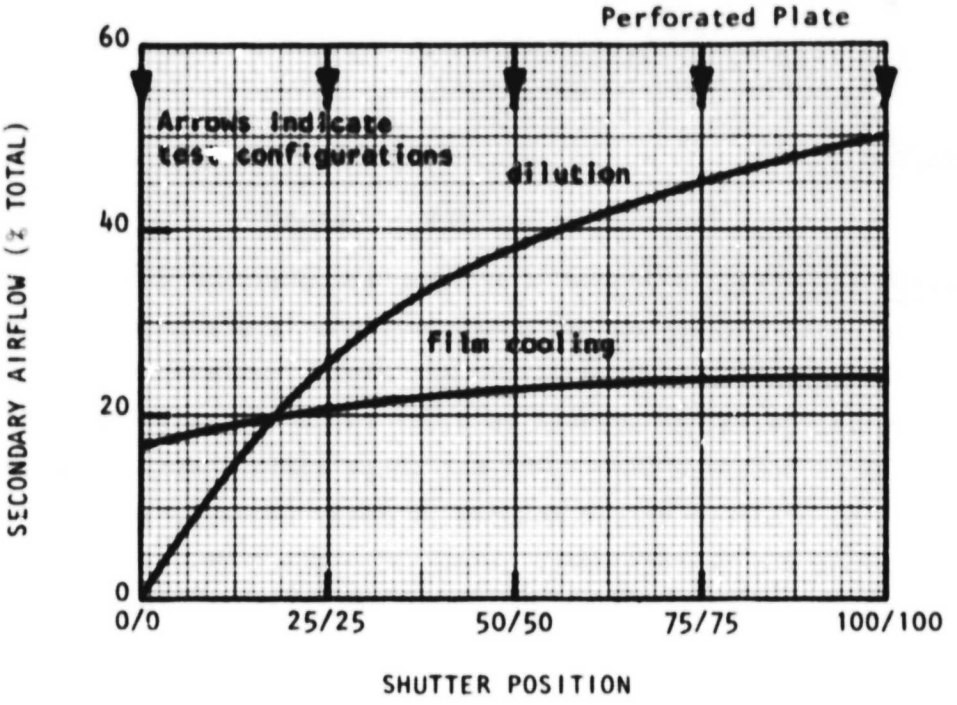

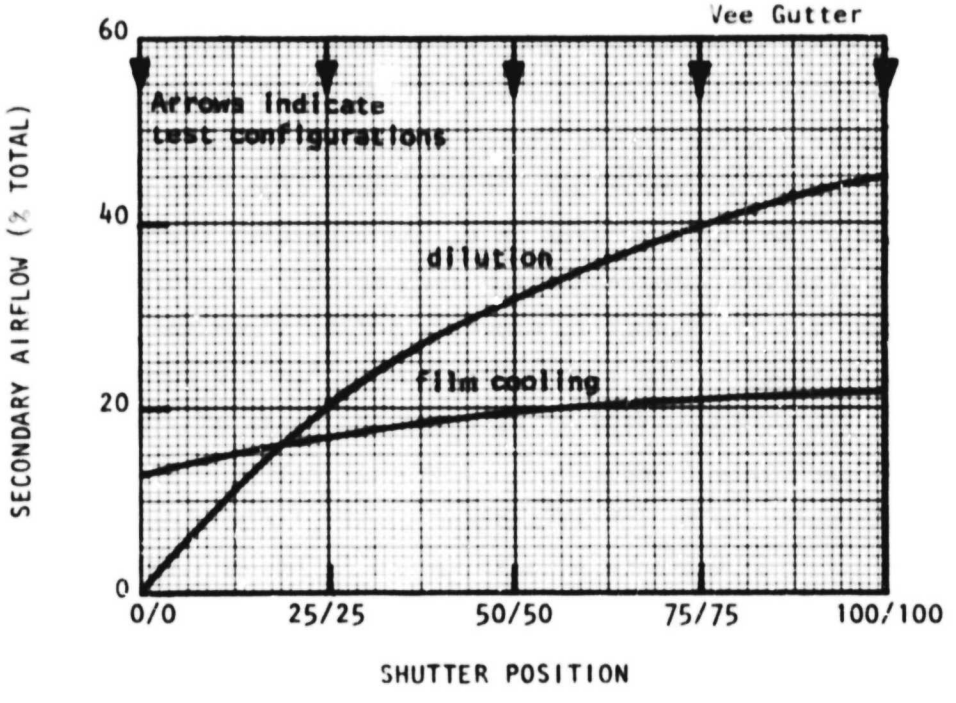

FIGURE 18. AIRFLOW SPLIT AS A FUNCTION OF DILUTION STAGING GEOMETRY

Perforated Plate - blockage 84%

Secondary Opening	$\frac{\dot{m}_{prim.}}{\dot{m}_{total}} = \frac{\phi_{overall}}{\phi_{prim.}}$	$\frac{\dot{m}_{cool.}}{\dot{m}_{total}}$	$\frac{\dot{m}_{dil.}}{\dot{m}_{total}}$	$\frac{\phi_{recirc.}}{\phi_{prim.}}$
0/0	0.83	0.17	0	0.72
25/25	0.53	0.21	0.26	0.79
50/50	0.39	0.23	0.38	0.85
75/75	0.31	0.24	0.45	0.85
100/100	0.26	0.24	0.50	0.82

Vee Gutter - blockage 69%

0/0	0.87	0.13	0	0.42
25/25	0.62	0.17	0.21	0.51
50/50	0.49	0.19	0.32	0.58
75/75	0.39	0.21	0.40	0.64
100/100	0.33	0.22	0.45	0.64

Cooling Area — 16 holes + 6 slots — 591mm^2 (Fixed) + 0 to 2155mm^2 (Variable)

Dilution Area — 12 slots — 0 to 5613mm^2 (Variable)

TABLE I. SUMMARY OF AIRFLOW SPLITS

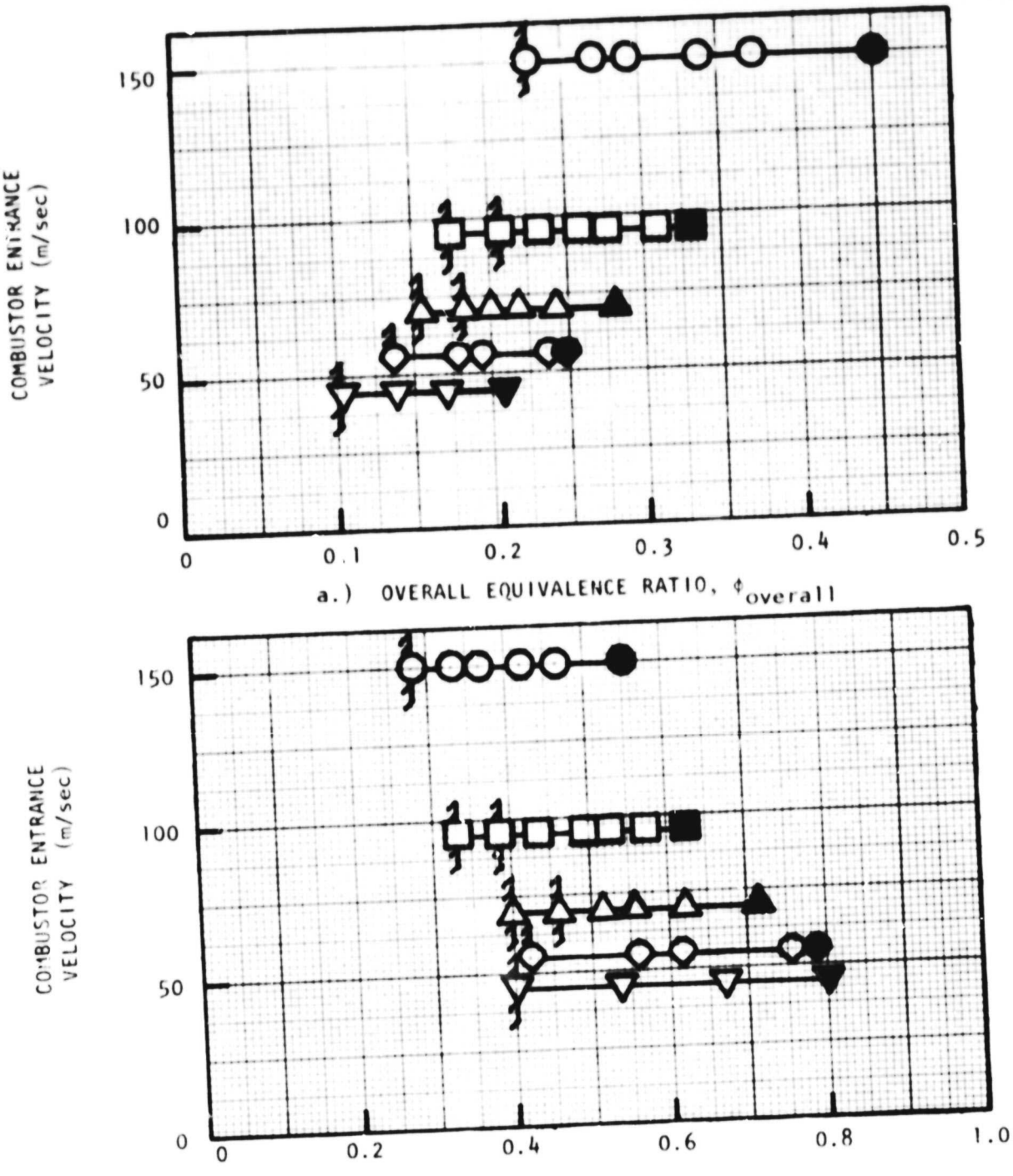

FIGURE 19. STABILITY LIMITS FOR THE PERFORATED PLATE FLAMEHOLDER.

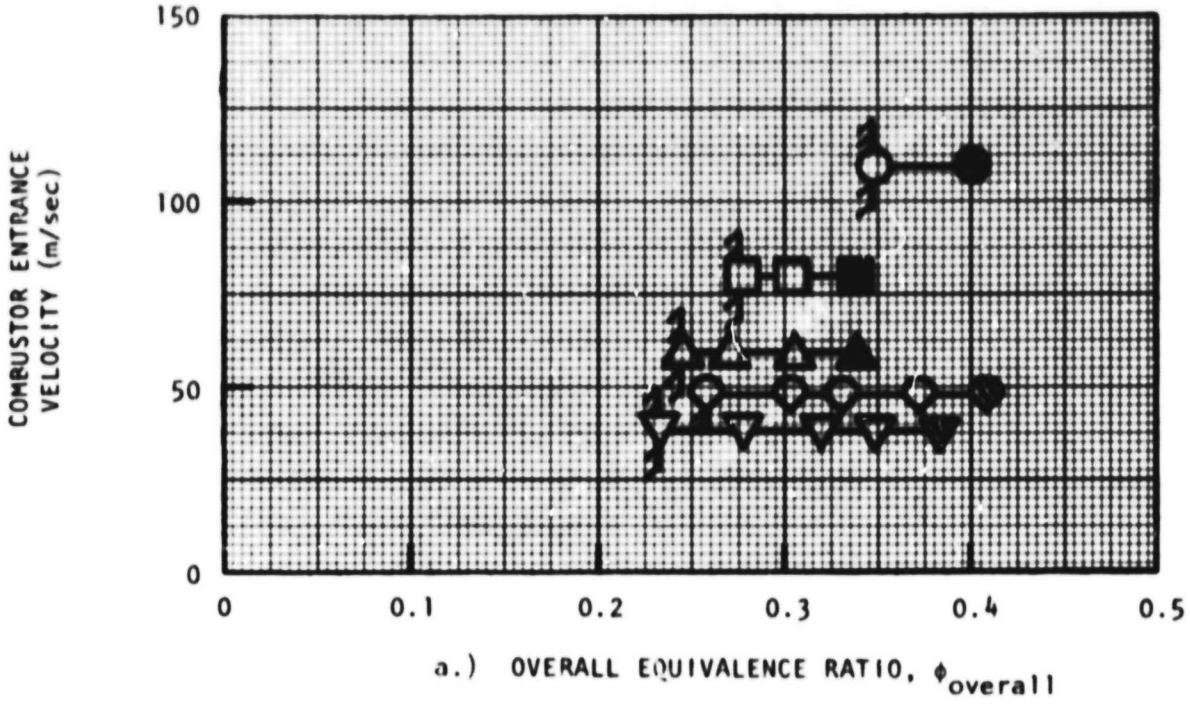

a.) OVERALL EQUIVALENCE RATIO, $\phi_{overall}$

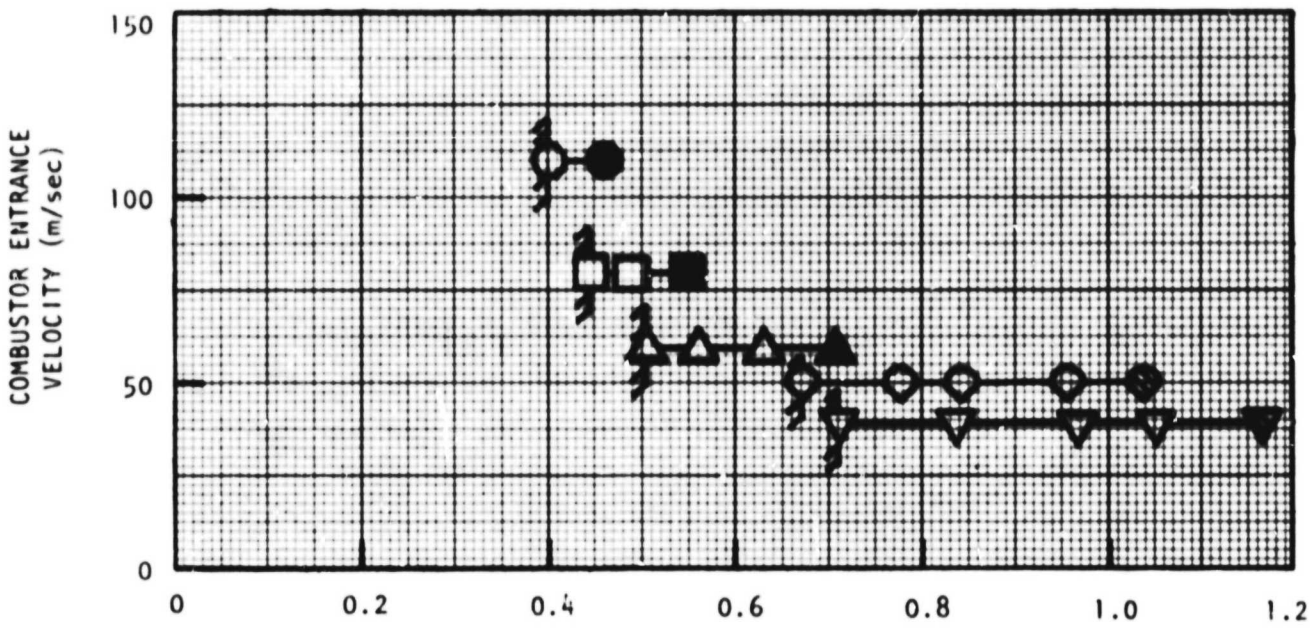

b.) PRIMARY ZONE EQUIVALENCE RATIO, $\phi_{primary}$

○ - 0% Dil. Air (0/0); □ - 21% Dil. Air (25/25); △ - 32% Dil. Air (50/50) (25/75); (75/25)

◇ - 40% Dil. Air (75/75); ▽ - 45% Dil. Air (100/100); ≀ - Indicates LSL;

● - Solid Symbol Indicates Flashback;

⊘ - Shaded Symbol indicates High Temp. Limit (No Flashback).

FIGURE 20. STABILITY LIMITS FOR THE VEE GUTTER FLAMEHOLDER.

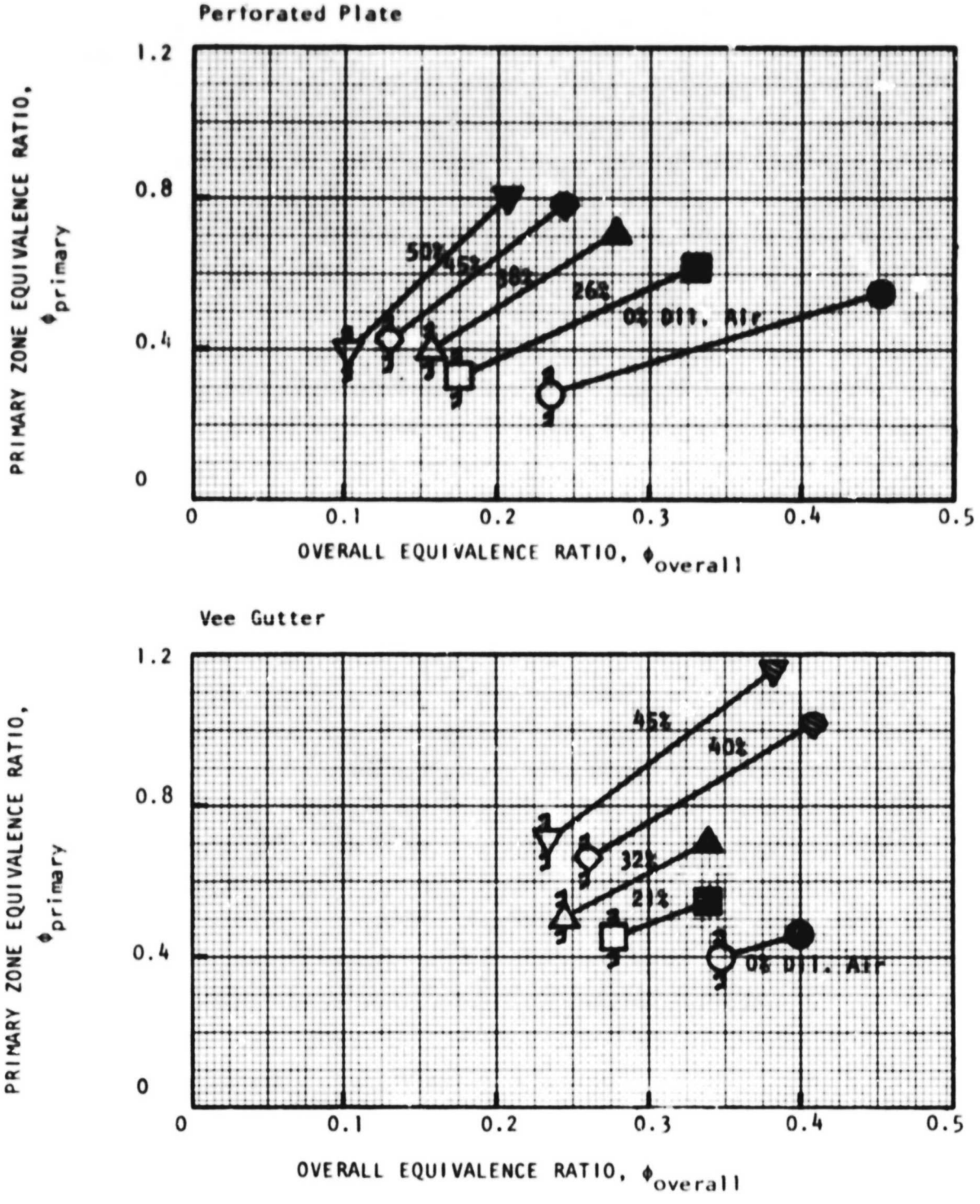

FIGURE 21. STABILITY SUMMARY FOR THE PERFORATED PLATE AND VEE GUTTER FLAMEHOLDERS.

of equivalence ratio (both overall and primary zone) at which flashback occurred. In some cases, multiple lean stability limit points are shown for a single value of combustor entrance velocity. This indicates the degree of variation observed in repeated tests.

Figure (19a) presents the stability limits for the perforated plate configuration in terms of overall combustor equivalence ratio. Here, increasing the combustor entrance velocity is seen to increase the range of equivalence ratio over which stable operation can be achieved. Lean stability limit equivalence ratio and flashback equivalence ratio are both linearly increasing functions of the combustor entrance velocity. Figure (19b) presents the same stability limits, this time plotted as functions of primary zone equivalence ratio. It can be seen that the primary zone equivalence ratio at the lean stability limit is a far weaker function of combustor entrance velocity than was overall equivalence ratio. Increasing combustor entrance velocity causes lean blowout to occur at lower primary zone equivalence ratios. On the other hand, increasing the combustor entrance velocity causes flashback to occur at lower primary zone equivalence ratios.

Figure (20) illustrates the range of the stable operation using the vee gutter flameholder. While the dependence of lean stability limit equivalence ratio (both overall and primary zone) on combustor entrance velocity is qualitatively similar to that observed for the perforated plate configuration, the sensitivity of the function is far greater. The flashback limits display a trend reversal in Figure (20a) which was not observed using the perforated plate flameholder. Aside from the nature of the trends displayed, the absolute values of stable operating equivalence ratio vary considerably for the two flameholders. The perforated plate displays primary zone lean stability limit equivalence ratios varying between 0.3 and 0.4, while the vee gutter displays primary zone lean stability limit equivalence ratios varying from 0.4 to 0.7.

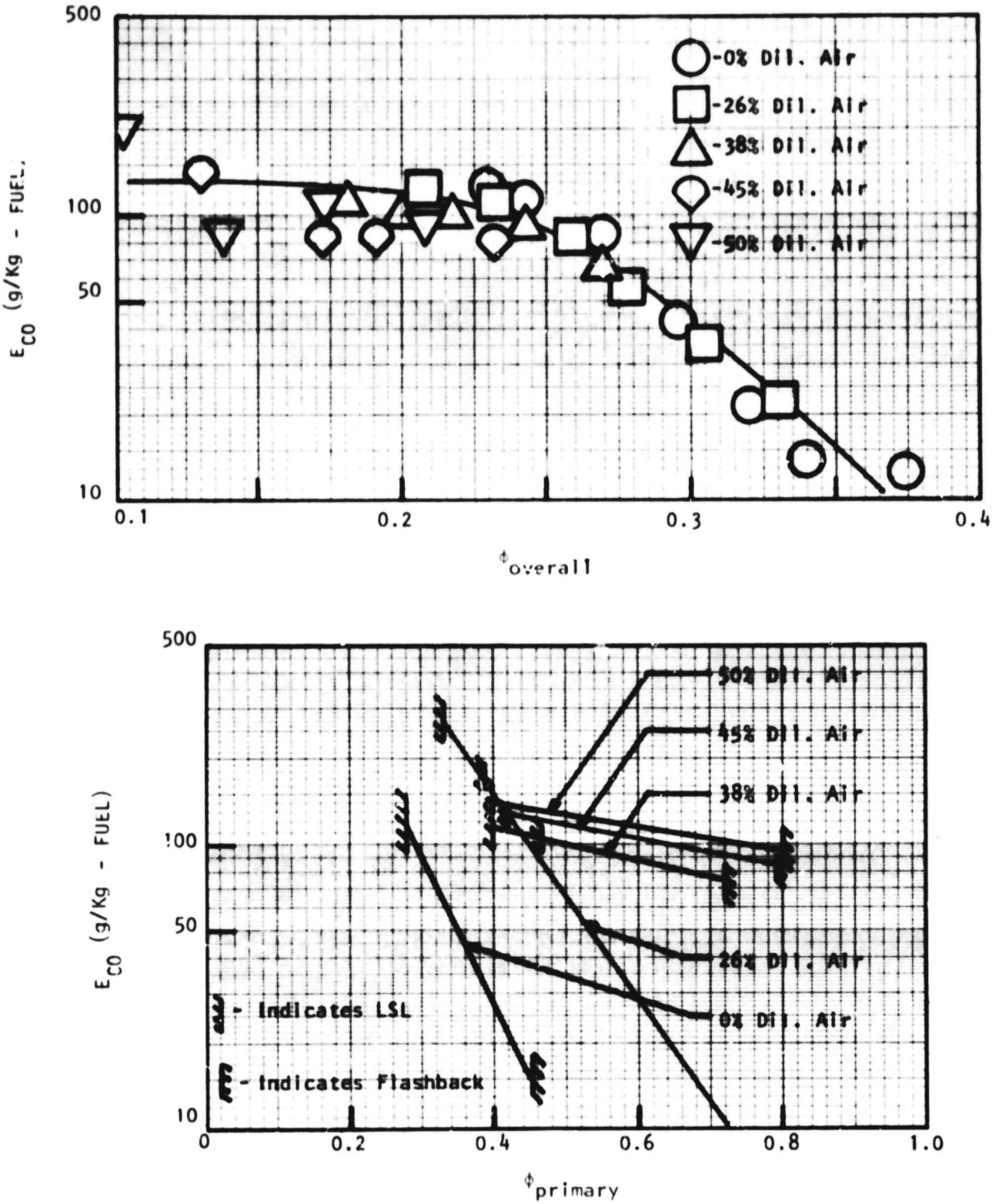

FIGURE 22. CO EMISSIONS FOR PERFORATED PLATE FLAMEHOLDER WITH SYMMETRIC DILUTION STAGING CONFIGURATIONS

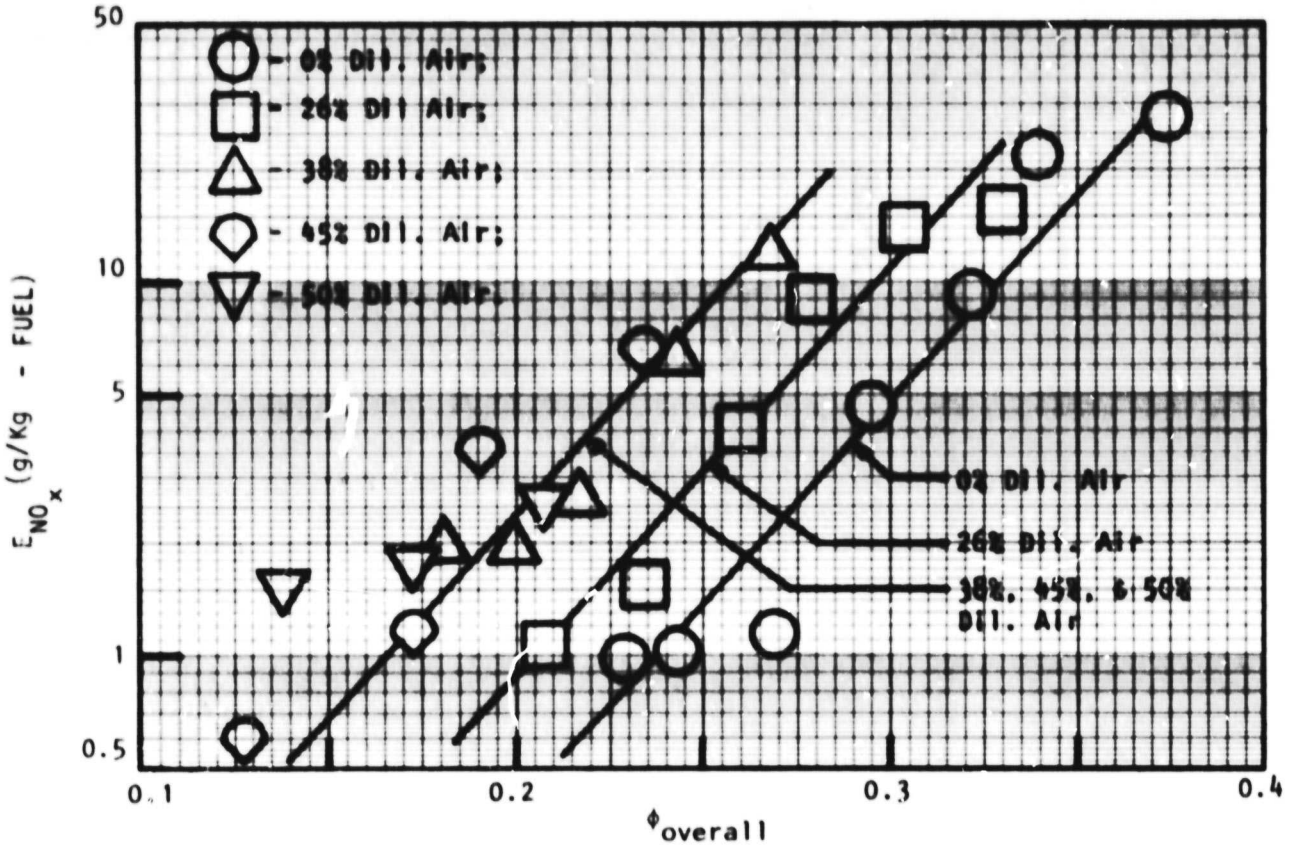

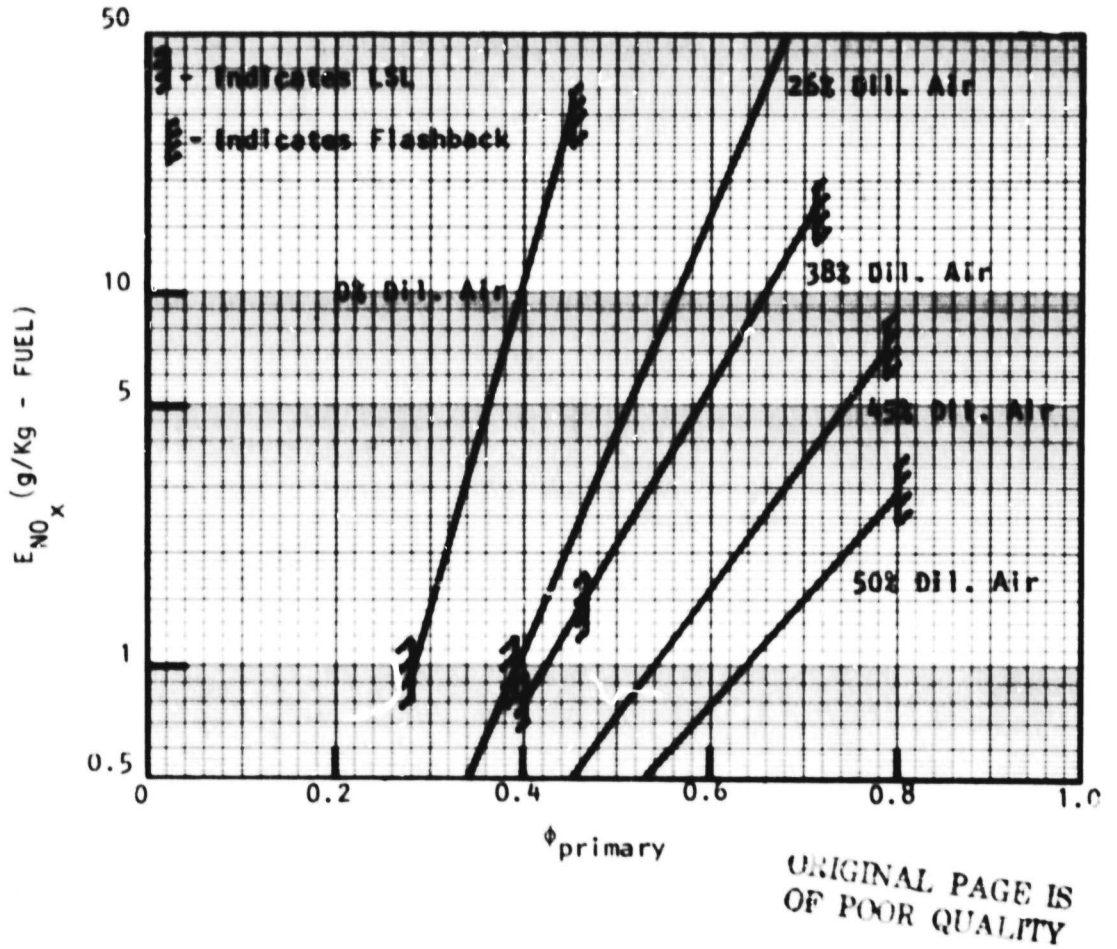

FIGURE 23. NO_x EMISSIONS FOR PERFORATED PLATE FLAMEHOLDER WITH SYMMETRIC DILUTION STAGING CONFIGURATIONS.

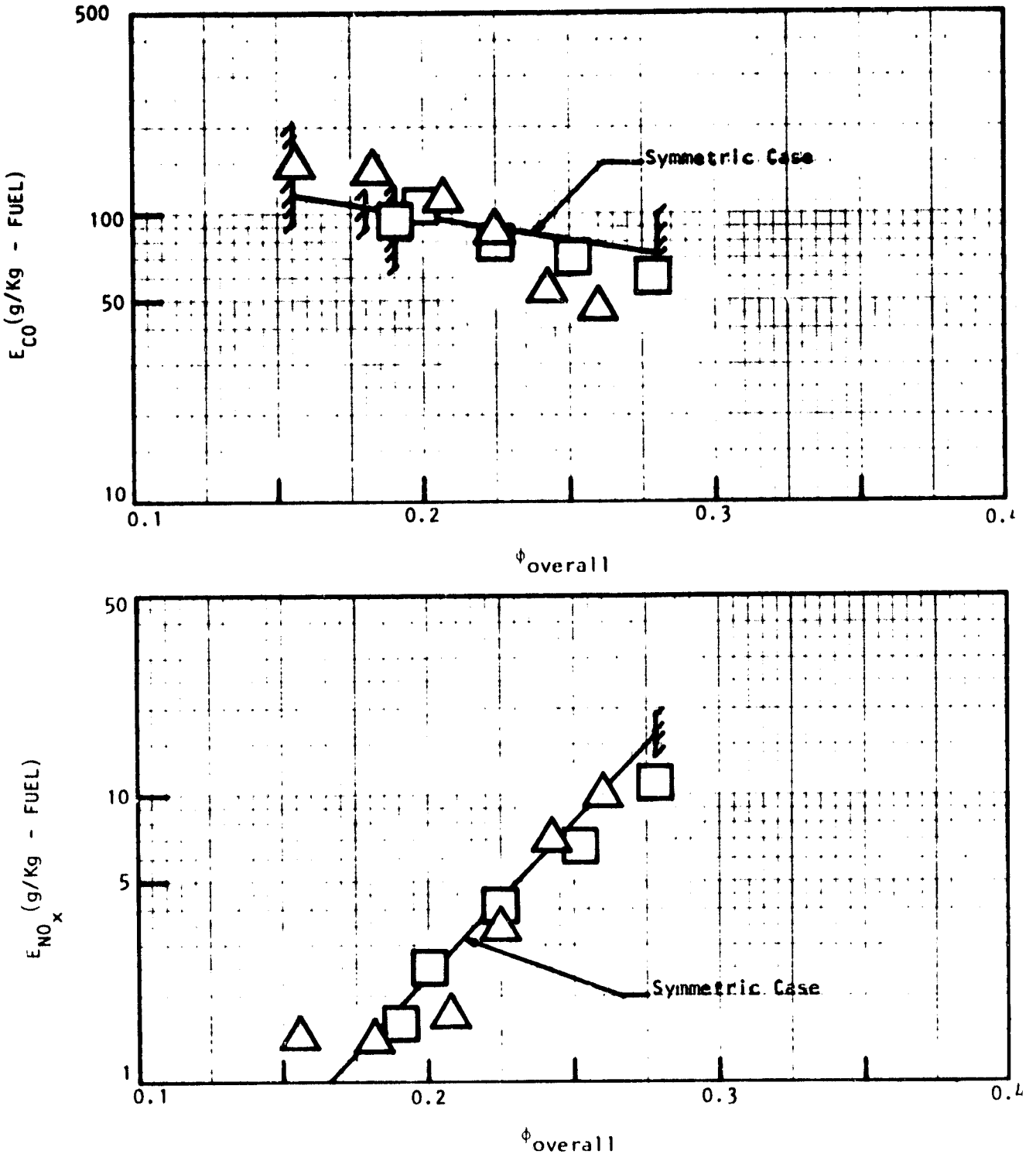

□ - 0% Dil. Air I Stage and 38% Dil. Air II Stage;

△ - 38% Dil. Air I Stage and 0% Dil. Air II Stage;

Sym. Case: 19% Dil. Air I Stage and 19% Dil. Air II Stage.

FIGURE 24. EFFECT OF NON-SYMMETRIC DILUTION STAGING ON THE EMISSIONS FOR THE PERFORATED PLATE FLAMEHOLDER

The stability characteristics of a given design were not affected by the details of the dilution zone geometry as long as the total open area of the dilution shutters was the same. Thus, the stability characteristics of the 50/50 geometry were the same as those of the 75/25 and 25/75 configurations. These results are also summarized in Figure (21).

Emissions - The emissions characteristics of the perforated plate configuration are presented in Figures (22) through (24). In Figure (22), the CO emissions characteristics appear to be a function of overall equivalence ratio (as opposed to primary zone equivalence ratio) displaying little sensitivity to the specifics of dilution zone geometry. CO emissions levels are quite high at overall equivalence ratios less than approximately 0.25 but become a rapidly decreasing function of equivalence ratio beyond that point.

Figure (23) shows NO_x to be a function of both overall and primary zone equivalence ratios. Here, the NO_x emission index is seen to increase logarithmically as overall equivalence ratio increases for a fixed level of dilution flow. For a fixed primary zone equivalence ratio, increasing the amount of dilution air reduces NO_x level.

Figure (24) illustrates the effect of dilution zone geometry on both NO_x and CO emissions for the perforated plate design by comparing the emissions obtained for asymmetric dilution air injection with those obtained for symmetric injection. The three cases all employ a total of 38% dilution air. It is clear from the figure that injecting the dilution air all in the first stage, all in the second stage, or half and half, has very little effect on the emissions of either NO_x or CO.

No significant emissions of unburned hydrocarbon species were detected for any stable operating mode utilizing the perforated plate flameholder. Hydrocarbon emissions were always detected at the lean stability limit but these emissions were extremely large, appeared quite suddenly and corresponded to flame extinction.

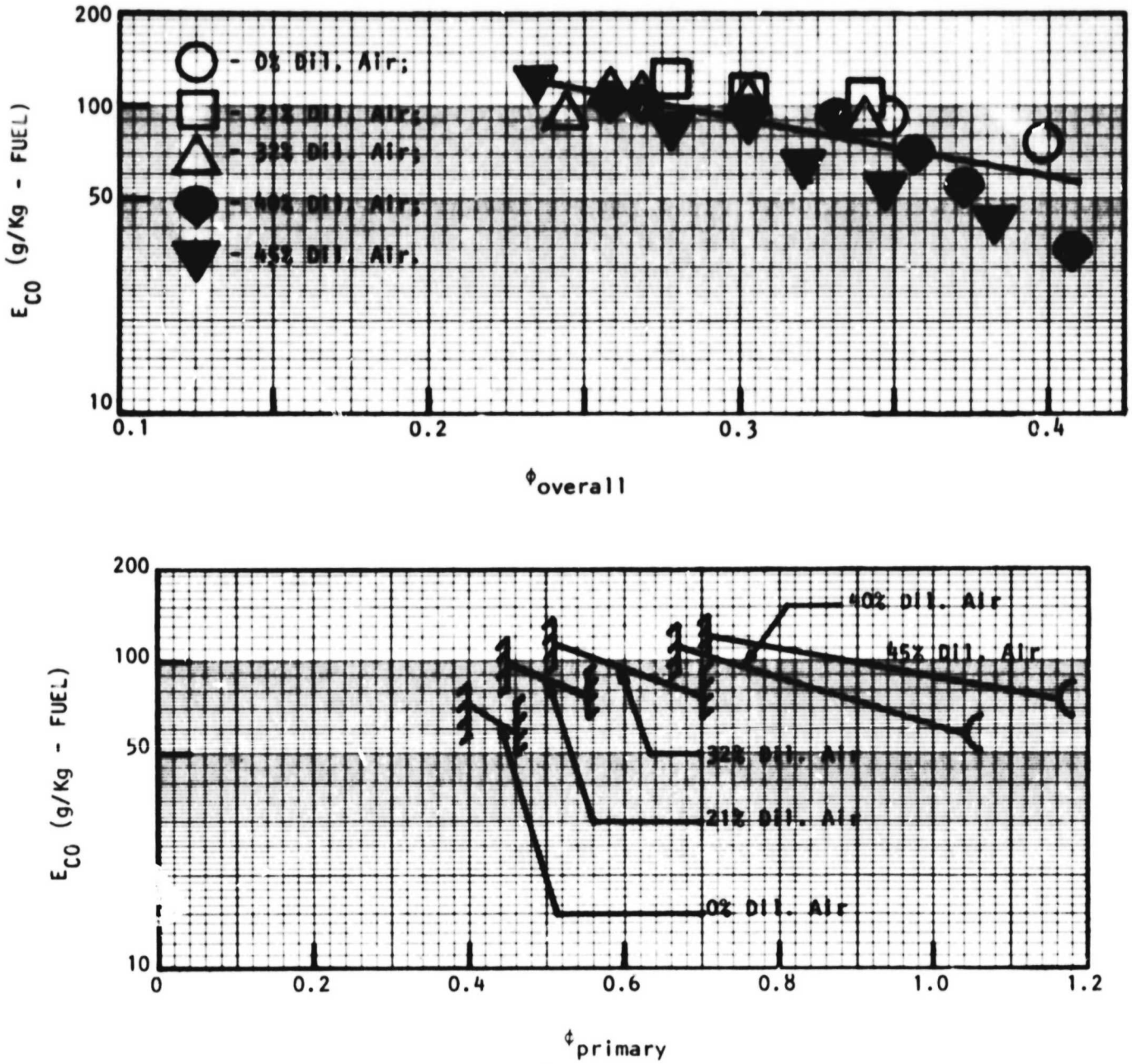

- Indicates LSL;

- Indicates Flashback;

- Indicates High Temp. Limit (No Flashback.)

FIGURE 25. CO EMISSIONS FOR VEE GUTTER FLAMEHOLDER WITH SYMMETRIC DILUTION STAGING CONFIGURATIONS.

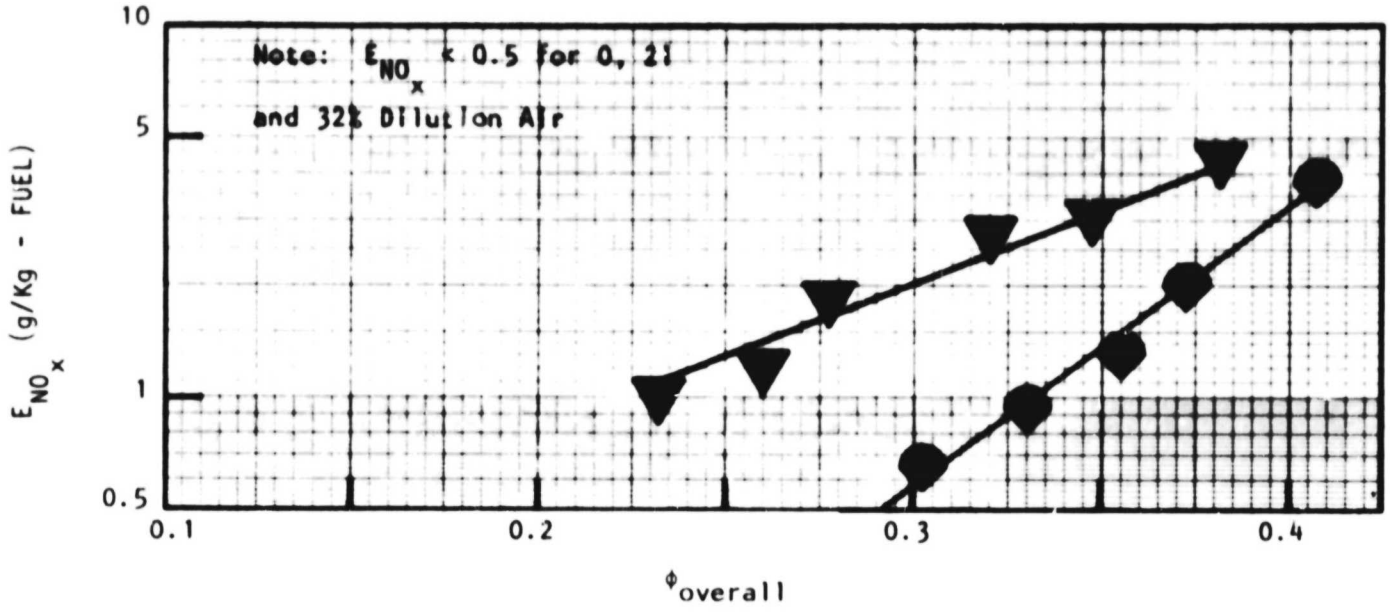

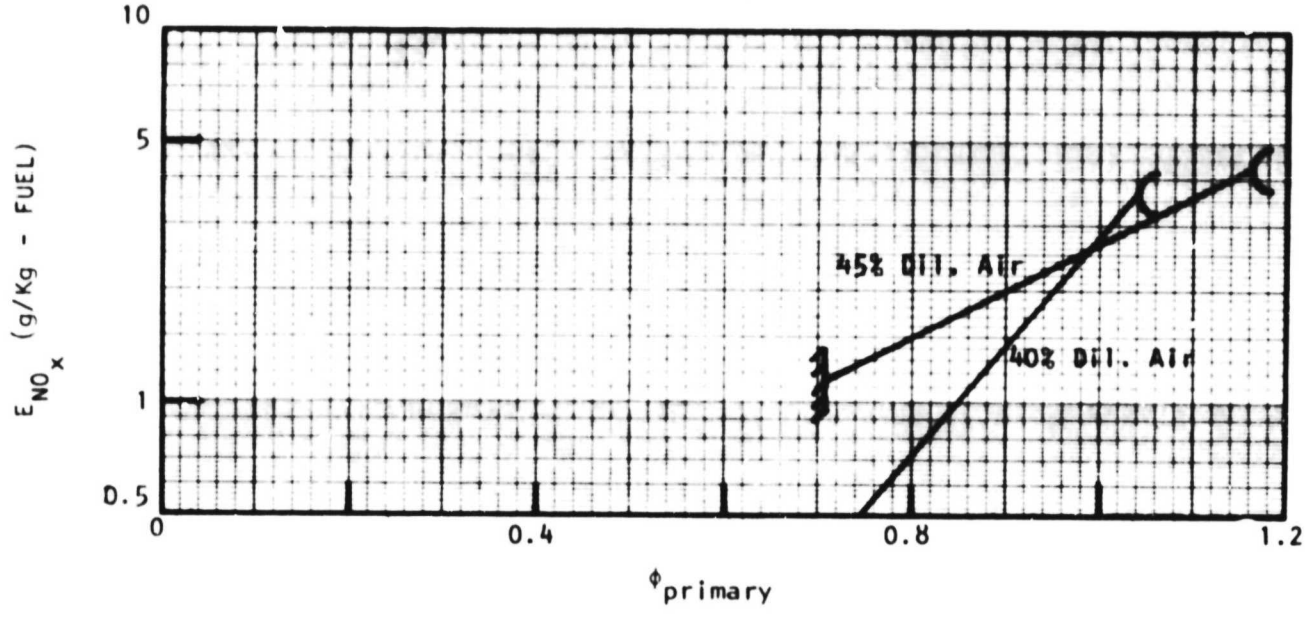

- 40% Dil. Air;
- 45% Dil. Air;
- Indicates LSL;
- High Temp. Limit (No Flashback.)

FIGURE 26. NO_x EMISSIONS FOR THE VEE GUTTER FLAMEHOLDER WITH SYMMETRIC DILUTION STAGING CONFIGURATIONS.

The carbon monoxide and NO_x emissions obtained using the vee gutter configuration are presented in Figures (25) and (26). Data represented by open symbols in these figures correspond to dilution air levels less than or equal to 32%. For these cases, although combustion could be maintained, it was characterized by substantial emissions of unburned hydrocarbons (beyond the capability of the exhaust gas analysis system to analyze accurately), substantial emissions of CO, and NO_x levels which were extremely low. Although combustion at these conditions was stable in the narrowest sense of the word, it could not be considered practical from an engineering viewpoint. The CO emissions levels presented in Figure (25) for dilution air levels of 40% and 45%, the only essentially stable operating conditions, are qualitatively similar to the data obtained using the perforated plate, with emission index correlating well as a function of overall equivalence ratio.

Figure (26) presents the corresonding NO_x levels. NO_x emissions for dilution air levels less than 40% were below 0.5 g/kg-fuel and do not appear on the figures. As with the perforated plate, increasing overall equivalence ratio at a fixed value of dilution airflow increases NO_x emissions. In contrast with the perforated plate characteristics, however, increasing dilution airflow at a fixed level of primary zone equivalence ratio increases NO_x level.

Combustion Testing - Jet-A

Two versions of the Jet-A air blast fuel injection assembly were tested. The first introduced fuel into the venturi throats through orifices mounted flush with the venturi walls. Attempts to achieve stable operation with this design were unsuccessful. In an effort to diagnose the problem, water was introduced through the fuel injection assembly in a cold flow test and operation of the injector was observed using the plexiglass sidewalls employed in the flow visualization tests. The injected liquid streams could be seen to reattach to the venturi walls a short distance downstream from the injection orifices. The liquid then flowed downstream along the

walls of the venturi diffuser collecting at the base of the assembly and formed large drops which eventually detached from the injector base and fell to the lower wall of the mixprep section. This reattachment of the injected liquid jets resulted in very little atomization, no prevaporization and an extremely poor distribution of fuel entering the combustion chamber.

The injector assembly was modified to eliminate this problem by extending the fuel delivery tubes to the centers of the venturi passages. Water tests of this design yielded relatively fine sprays for the condition of zero dilution (maximum velocity through the injector device) but spray quality was poor at dilution conditions where the air velocity through the injector was reduced. Combustion tests utilizing this second injector design showed the device to be only marginally stable. Ignition was quite difficult and could only be accomplished using a hydrogen-fueled diffusion torch in the combustor primary zone. Reducing the fuel flow to this torch produced noisy combustion which generally led either to flame extinction or flashback, depending upon the equivalence ratio of the system. There was an extremely narrow range of equivalence ratio over which combustion could be sustained, but minor changes to operating variables would usually cause pressure oscillations and flashback. It should be noted that the range of primary zone equivalence ratio over which stable operation could be achieved was relatively narrow even when the combustor was fueled with propane. Coupling the effects of combustor pressure oscillations on vaporization and mixing of the Jet-A fuel and air clearly exascerbates the stability problem by causing increased fluctuations in primary zone gas-phase equivalence ratio. The extremely narrow range of operation made it impossible to obtain meaningful emission data with this configuration.

DISCUSSION

This section presents a discussion of the experimental results and is divided into subsections dealing with the specific effects of secondary air entrainment by the flameholders, lean stability and flashback limits and emissions of carbon monoxide and NO_x.

Entrainment of Secondary Air by the Flameholder

Although centerplane streamline tracings indicate that the reverse flow regions behind the perforated plate flameholder do not extend sufficiently far downstream to encompass the first dilution or the first film cooling slot, the fuel content of the recirculating gas has been found to be diluted to between 72% and 85% of its incoming value, depending upon staging configuration. The mechanism through which entrainment occurs is not well defined. One possible explanation is that local recirculating flows extend further downstream in the planes which do not contain flameholder perforations than they do in the centerplane (which contains a row of combustor entrance jets). Entrainment of secondary air is greatest when the combustor entrance velocity is greatest and the recirculation zones have their greatest streamwise extent. Interestingly, at the condition of maximum secondary air entrainment, the dilution air slots are entirely closed and entrained air can only come from the first film-cooling slot.

The centerplane streamline tracings for the vee gutter flameholder configuration show the triangular planform recirculation zone to encompass approximately half the width of the first film cooling slot and part of the center slot of the first dilution stage. In this case, secondary air entrainment in the flameholder recirculation zone is approximately twice that of the perforated plate. As before, entrainment is greatest when combustor entrance velocity is greatest. The condition of maximum secondary air entrainment corresponds to the 0/0 configuration in which the dilution slots are entirely closed. Clearly then, the entrained air is captured from the first film-cooling slot. The amount of film cooling air which is captured is sufficient to dilute the fuel content of the recirculation zone to just over 40% of its incoming value. Opening the first dilution stage allows air to flow directly into the recirculation zone from the center dilution slot. At the same time, the increased combustor entrance area reduces combustor

entrance velocity and, correspondingly, the strength of the flameholder vortex system entraining less film cooling air. The fact that net secondary air entrainment decreases when the dilution slots are opened implies that the entrainment of film cooling air dominates the vee gutter flameholder entrainment process.

For each flameholder, staging configurations 25/75, 50/50, and 75/25 produce the same combustor entrance velocity and film-cooling airflow rate but significantly different downstream flowfields. Nevertheless, these configurations all produce the same degree of secondary air entrainment. The inescapable conclusion here is that most of the air entrained by both flameholders is film cooling air from the first cooling slot and that the degree of entrainment depends upon the streamwise extent of the recirculation zones and the combustor entrance velocity through its influence on the strength of the attached vortices.

Lean Stability Limit

Radhakrishnan et al (Reference 3) present a review of lean stability limit data for premixed combustion stabilized by recirculating flows and conclude that the equivalence ratio at lean blowout is an increasing function of combustor entrance velocity. A model, based in part on this observation, is used to predict the variation of equivalence ratio at lean blowout with combustor entrance velocity and matches flame-tube test data for a perforated plate flameholder quite well.

Comparing the present experiment with this prediction is complicated by the fact that the equivalence ratio is not single-valued as it is in flametube experiments. Here, a number of equivalence ratios can be defined, principal among these:

i) equivalence ratio in the primary zone (mixprep duct exit) gases

ii) equivalence ratio in the flameholder recirculation region

iii) overall equivalence ratio

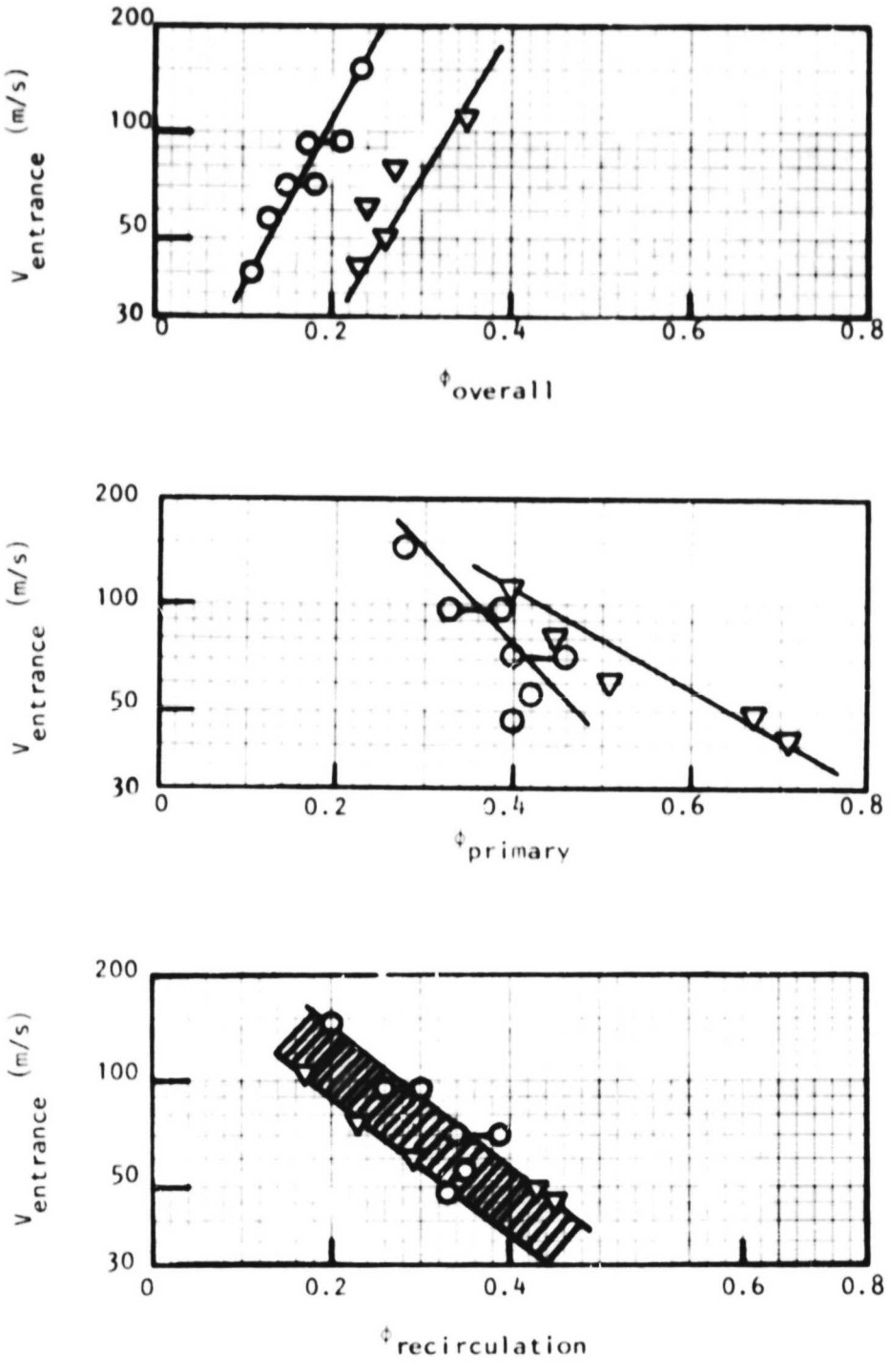

FIGURE 27. EQUIVALENCE RATIOS AT THE LEAN STABILITY LIMIT.

Figure (27) presents the measured equivalence ratios at the lean stability limit as functions of combustor entrance velocity for both flameholder designs. Overall equivalence ratio is the only one of the three which displays the trend predicted in Reference 3. However, the values of overall equivalence ratio observed at the lean stability limit are far lower than flame-tube experiments (References 4 and 5 e.g.) would lead one to anticipate and the behavior of the perforated plate and vee gutter designs is significantly different, a result in conflict with the observations of Reference 4. Further, since much of the airflow included in the computation of overall equivalence ratio enters the combustor at points far removed from the flame stabilization zone, it is difficult to make a physical argument supporting the significance of this parameter.

The magnitude of the primary zone equivalence ratio for the perforated plate at lean blowout is in the range which might be expected based on flame-tube results but the vee gutter primary zone equivalence ratios at blowout are, again, significantly different and far higher than would be anticipated. Since the vee gutter entrains far more secondary air in its recirculation zone than the perforated plate, one might expect this to be the reason for the difference. The trend with combustor entrance velocity, however, is contrary to that predicted by Reference 3 and leads one to consider recirculation zone equivalence ratio as a possible governing parameter.

Unfortunately, recirculation zone equivalence ratio was not measured during combustion and can only be inferred by assuming that the degree of recirculation zone dilution measured in the cold flow tests is a reasonable measure of that which takes place under hot flow conditions. With the limitations of this assumption in mind, Figure (27) indicates that the behavior of the perforated plate and vee gutter designs look quite similar but the magnitude of the calculated equivalence ratio is still lower than one would expect as possible based on flame-tube data. The low values of blowout equivalence ratio could be a reflection of a poorly mixed system

at low fuel injection rates.

Summarizing, the data obtained here does not appear sufficient to identify one particular equivalence ratio as being responsible for the lean stability phenomenon. It is possible that the lean blowout point is determined by a combination of primary zone and recirculation zone equivalence ratio, reflecting the physical nature of the mixing process which produces ignition. If this is so, the stabilizing effect of velocity may come through its effect on the rate of mixing between the primary and recirculation zone gases.

Flashback

The phenomenon of flashback was studied in Reference (6) in a lean premixed flametube experiment where combustion was stabilized by a sudden expansion from the mixture preparation tube into a combustor. The results of this study indicate that the equivalence ratio at which flashback occurs is an increasing function of combustor entrance velocity. An examination of the flashback data for the perforated plate flameholder shows this trend if one considers "equivalence ratio" to be the overall equivalence ratio of the system. Although the complex interactions between primary and secondary airflows in this system makes a direct comparison of results with a flametube experiment difficult, it would appear that the flashback behavior of an LPP system is a function of overall equivalence ratio rather than equivalence ratio at the combustor entrance station.

The flashback data obtained for the vee gutter configuration is more difficult to interpret. Here, the three lower values of dilution air level produced flashback while the two highest levels of dilution air (the two truly stable configurations) did not. It is possible that the flashback observed for the less stable configurations was connected with periodic pressure fluctuations which these configurations experienced during operation. On the other hand, the ability of the vee gutter to operate at relatively high equivalence ratios without flashback at low combustor entrance velocities demonstrates that flameholder geometry and dilution can substantially affect the flashback characteristics of an LPP combustion system.

Carbon Monoxide Emissions

The data of Reference (7) indicate that a lean premixed system stabilized by a perforated plate flameholder should produce equilibrium CO levels in the primary zone if the primary zone residence time is at least 2.5 msec. In the present case, the minimum primary zone residence time is approximately 3 msec. Therefore, it must be concluded that the relatively high CO levels produced by the combustor, independent of flameholder geometry, are the result of film cooling and dilution airflow interaction. Since high CO levels are observed at low overall equivalence ratios with no dilution airflow, the only secondary air common to all conditions is the (approximately) 20% of the total airflow used for liner film cooling. It is possible that the relatively cool conditions near the liner walls prevents CO from reaching equilibrium prior to the first film-cooling station. Past that point, the continued addition of cooling air slows local CO oxidation reactions sufficiently to produce the CO emissions measured. This is a particularly interesting result as it points out the sensitivity of a lean premixed combustion system to wall cooling interactions. This sensitivity results from the fact that an LPP system must, by definition, have as much fuel near the walls as exists in the central region of the combustor. The necessity to oxidize a portion of the fuel in the immediate vicinity of a wall automatically couples the CO emissions problem with the effectiveness of the wall cooling system.

NO_x Emissions

Previous studies in flametube combustors have indicated that the NO_x emission rate is a sensitive function of primary zone equivalence ratio and the results obtained here with the perforated plate flameholder configuration confirm that effect.* Although increasing the amount of bypass (dilution air) increases NO_x levels for a fixed overall equivalence ratio, this is simply a reflection of the resulting increase in primary zone equivalence ratio. For a fixed level of primary zone equivalence ratio, increasing the dilution

---

*The low combustion efficiency of the vee gutter configuration at dilution air levels below 45% makes it impossible to draw a direct conclusion on the separate effects of primary zone stoichiometry and dilution air quenching on NO_x production reactions.

airflow fraction decreases NO_x reflecting the quenching effect which the dilution air produces on the NO_x production reactions.

The insensitivity of NO_x emissions to dilution staging evidenced in Figure (24) implies that the NO_x production reactions in the three configurations represented in the figure continue well downstream of the dilution zone. The streamline traces for the three cases (Figures 13b, d and e) indicate that the dilution jet penetration pattern varies considerably. Therefore, it appears that the lateral mixing of the dilution jets with the primary zone effluent is the rate-determining factor and requires a reasonable distance to accomplish thorough mixing.

CONCLUSIONS

The flameholder recirculation zone of an LPP combustor can entrain both dilution and film-cooling air. A perforated plate flameholder with a relatively short near wake region entrains sufficient film cooling and dilution air to reduce the equivalence ratio in its near wake to between 72% and 86% of the incoming primary stream value, depending upon staging configuration. A vee gutter flameholder, whose near wake encompasses secondary air injection regions, entrains sufficient film cooling and dilution air to reduce its recirculation zone equivalence ratio to between 42% and 65% of the incoming primary stream value. Combustor entrance velocity appears to be the parameter which controls this phenomenon with increased entrance velocity producing increased entrainment.

Increasing primary zone entrance velocity increases resistance to flashback for a fixed overall equivalence ratio. Flashback may be more dependent upon overall equivalence ratio than upon local equivalence ratio in the combustor primary zone. Flameholder geometry has a pronounced effect on the flashback characteristics of the system.

The lean stability limit of an LPP combustor is a function of both primary zone equivalence ratio and equivalence ratio in the flameholder recirculation zone. Contrary to expectations, increasing the combustor primary zone entrance velocity increases resistance to lean blowout.

NO_x emissions are a sensitive and increasing function of primary zone equivalence ratio. For a fixed value of $\phi_{primary}$, increasing the amount of dilution air decreases NO_x emissions by quenching reactions. Quenching effectiveness depends only on total dilution air added; the specific geometry of the dilution zone has no observable effect.

CO emissions are a function of overall equivalence ratio and independent of dilution geometry. This implies that CO oxidation reactions are retarded near the cooled walls but go to completion in the mainstream of

the combustor. CO emissions decrease as overall equivalence ratio increases.

The axial position where dilution air was introduced had no observable effect on emissions or stability. Only the quantity of dilution air was important through its effect on primary zone stoichiometry.

REFERENCES

1. Dickman, R.A., Dodds, W.J. and Ekstedt, E.F., "Lean Premixed-Prevaporized (LPP) Combustor Conceptual Design Study," NASA CR-159629, August 1979.

2. Fiorentino, A.J., Green, W. and Kim, J., "Lean Premixed, Prevaporized Fuel Combustor Conceptual Design Study," NASA CR-159647, August 1979.

3. Radhakrishnan, K., Heywood, J. and Tabaczynski, R., "Premixing Quality and Flame Stability: A Theoretical and Experimental Study," NASA CR-3216, December 1979.

4. Roffe, G. and Venkataramani, K. S., "Experimental Study of the Effects of Flameholder Geometry on Emissions and Performance of Lean Premixed Combustors, " NASA CR-135424, June 1978.

5. McVey, J. B. and Kennedy, J. B., "Lean Stability Augmentation Study," NASA CR-159536, May 1979.

6. Marek, C. J. and Papathakos, L. C., "Preliminary Studies of Autoignition and Flashback in a Premixing Prevaporizing Flame Tube Using Jet-A Fuel at Lean Equivalence Ratios," NASA TM X-3526, 1977.

7. Roffe, G. and Venkataramani, K. S., "Experimental Study of the Effects of Cycle Pressure on Lean Combustion Emissions," NASA CR-3032, 1978.

8. "Procedure for the Continuous Sampling and Measurement of Gaseous Emissions from Aircraft Turbine Engines," Society of Automotive Engineers, ARP-1256, October 1971.

APPENDIX A

DATA REDUCTION PROCEDURES

The gas analysis instrumentation which is illustrated in Figure A1, provides raw data in the form of volume fractions of the particular gases being sampled. This raw data is converted into the more convenient form of emission index and equivalence ratio following the procedures detailed below.

Each of the gas analysis instruments must be calibrated in order to convert the instrument reading to the volume fraction of the particular gas being analyzed. In the case of the Beckman Model 402 hydrocarbon analyzer and the Beckman Model 315B CO analyzer, this calibration is accomplished by passing prepared mixtures of calibration gas through the instruments and establishing calibration curves. The hydrocarbon analyzer was calibrated using gas standards containig 47 ppm, 91 ppm, 114 ppm, and 269 ppm propane in nitrogen. The instrument output is proportional to the number of carbon atoms with hydrogen bonds. Thus, pure hydrogen or pure carbon will produce no response and a given concentration of propane (C_3H_8) will produce three times the response of an equal concentration of methane (CH_4). The instrument responds to all C-H bonds. As a result, it measures the sum of both unoxidized hydrocarbon and partially oxidized hydrocarbon molecules. The response is linear with hydrocarbon concentration, presented in units of ppmC, that is, the number of hydrogenated carbon atoms in parts per million.

Calibration of the Beckman Model 315B CO analyzer was accomplished using standard gases with 1530 ppm, 1043 ppm, 605 ppm, and 65 ppm CO in nitrogen.

The gases used for calibration of the Beckman Model 864 CO_2 analyzer contained 10.2%, 5. % and 2.0% CO_2 in nitrogen. The TECO Series 10 NO/NO_x analyzer was calibrated using standards containing 250 ppm, 104 ppm and 21 ppm NO_x in nitrogen.

The gas analysis instruments were calibrated once each week using the entire set of standard gases. Zero gas and span gas were passed through all instruments immediately prior to each test and the instrument output

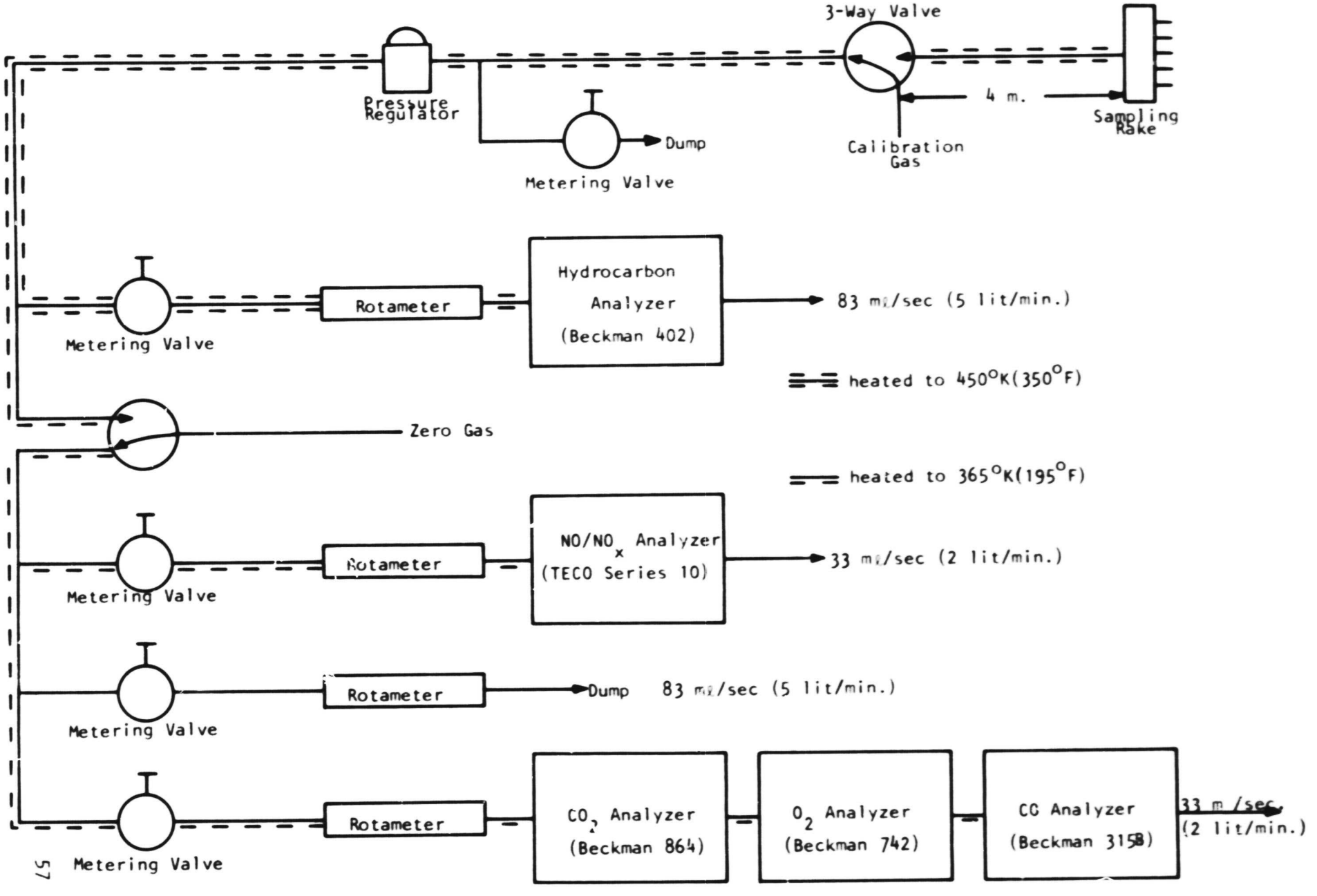

FIGURE A1. SAMPLING SYSTEM SCHEMATIC

recorded on the same data roll which was used for the subsequent test run.

Conversion of the molar concentration (volume fractions) provided by the gas analysis instrumentation into the more convenient terms of emission index and equivalence ratio requires a prior knowledge of the ratio of carbon to hydrogen in the system. This is ascertained from a chemical analysis of the fuel used in the experiments. For propane, the fuel used here, the hydrogen to carbon ratio is 2.67 and the fuel/air ratio f/a is given by Reference (8) to be

$$f/a = \frac{CO \times 10^{-4} + CO_2 + HC \times 10^{-4}}{197.7 - 2.31 \times 10^{-4}\ CO - 1.32\ CO_2} \qquad (A1)$$

where CO and HC are the molar concentrations of carbon monoxide and unburned hydrocarbon in units of parts per million (ppm) and ppmC respectively and CO_2 is the volume percent of carbon dioxide expressed as a percentage of total gas volume.

The equivalence ratio ϕ, is defined as the ratio of the actual fuel/air ratio to the stoichiometric fuel/air ratio. For propane

$$\phi = (f/a) / 0.064 \qquad (A2)$$

The measured volume fractions expressed as ppm of CO, hydrocarbons, and NO_x, are converted into emission indices (grams of component per kilogram of fuel) using the following expressions:

$$E_{CO} = \frac{CO\ (1 + f/a)}{1035\ f/a} \qquad (A3)$$

$$E_{HC} = \frac{HC\ (1 + f/a)}{1975\ f/a} \qquad (A4)$$

$$E_{NO_x} = \frac{NO_x\ (1 + f/a)}{630\ f/a} \qquad (A5)$$

In Equation (A5), the molecular weight of NO_x is taken to be 46. This reflects the assumption that all NO produced eventually becomes NO_2. The emission index is thus based on the molecular weight of the NO_2 molecule.